Naval Research Reviews

Office of Naval Research
Summer 1981
Vol XXXIII No. 3

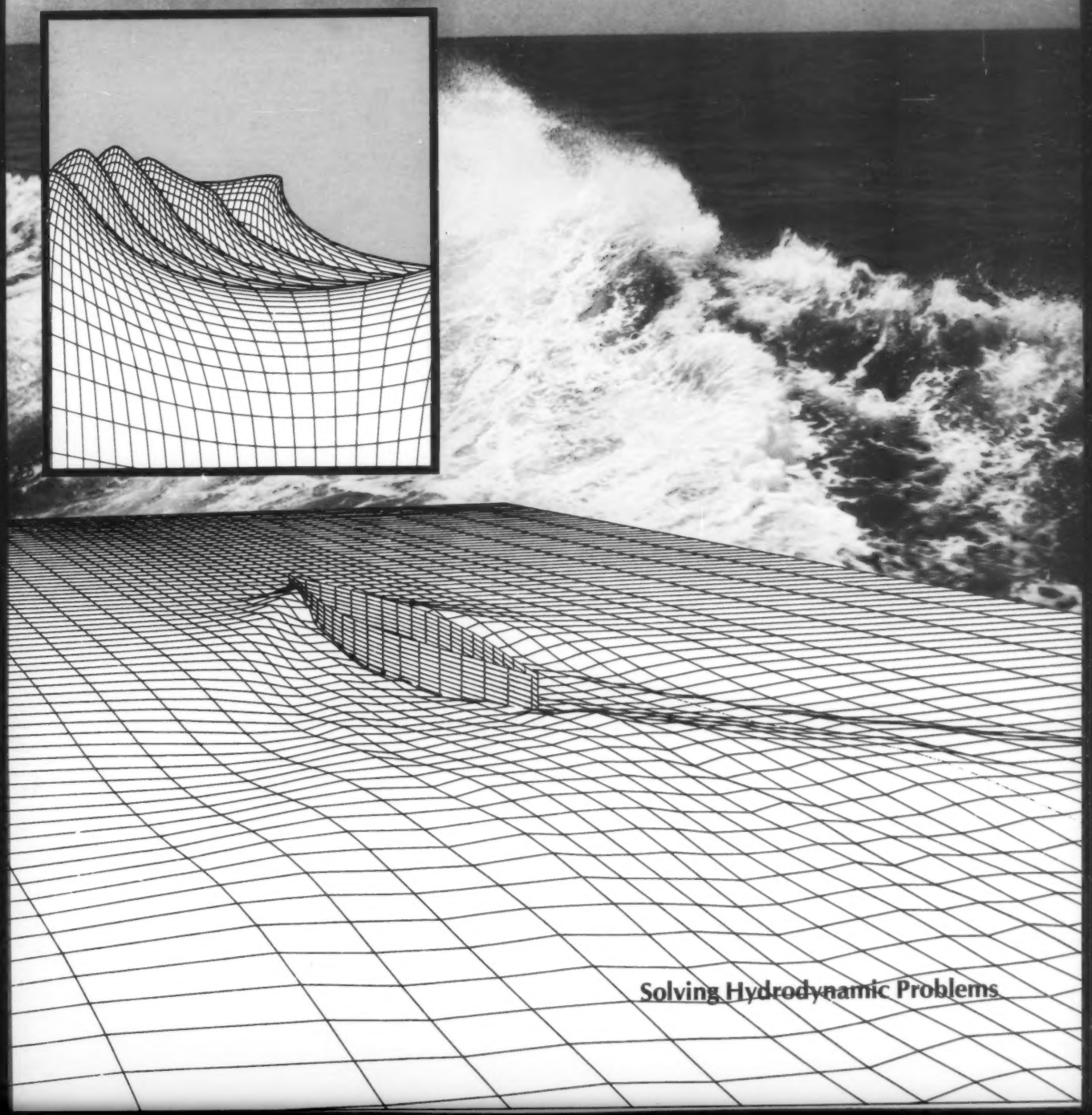

Solving Hydrodynamic Problems

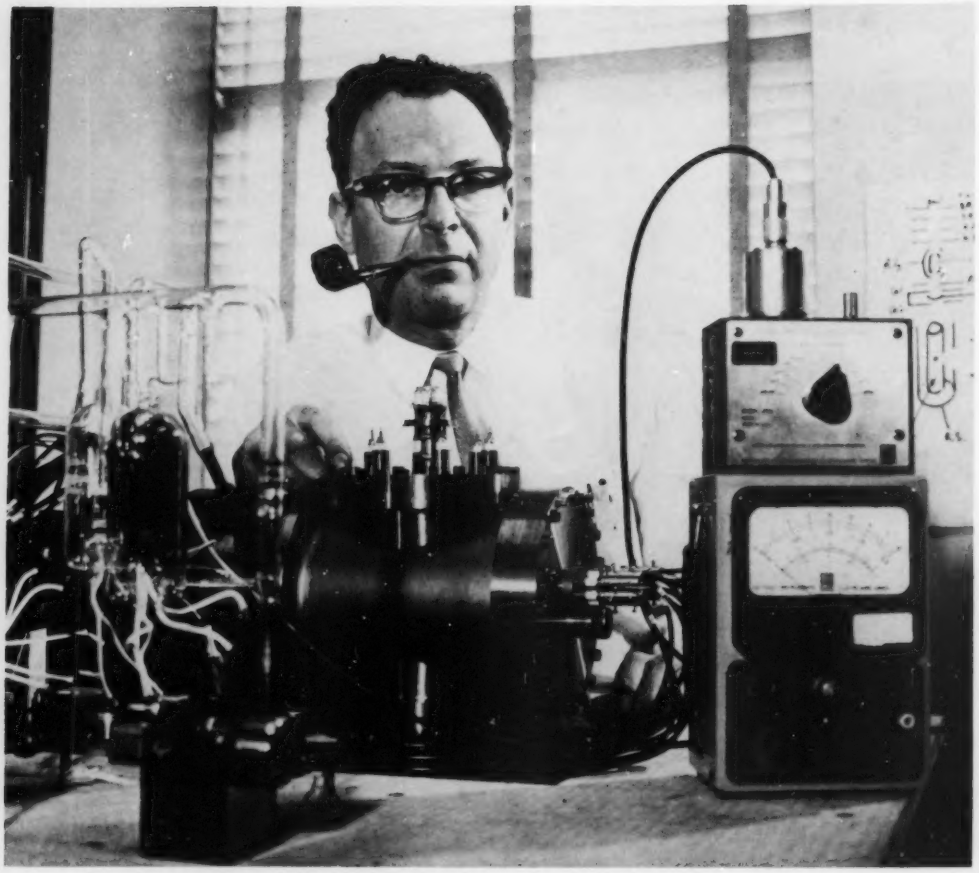

The late Professor George J. Schulz in his laboratory at Yale shortly after winning the first Davisson-Germer prize in 1965 for his outstanding work in atomic physics. He was honored for being the first to observe helium resonance in the elastic scattering cross section of electrons from helium atoms. This new discovery opened up the whole field of resonant electron scattering from atoms and molecules which has had tremendous impact on the understanding of e-atom, e-molecule interactions and subsequently helped in the development of gaseous lasers. This research was conducted by Professor Schulz under the support of the Office of Naval Research.

Naval Research Reviews

Office of Naval Research
Summer 1981
Vol XXXIII No. 3

Chief of Naval Research	RADM L.S. Kollmorgen, USN
Technical Director	Dr. J.A. Smith
Scientific Editor	Dr. G.A. Neece
Assistant Editor	Dr. J.T. Lester
Assistant Editor	Dr. D.A. Patterson
Managing Editor	M.J. Whetstone
Chief Writer/Editor	W.J. Lescure, III
Art Director	Edward Bailey

ARTICLES

3 Five Years of Numerical Naval Ship Hydrodynamics at DTNSRDC
by Nils Salvesen

20 An Optical Method for Measuring the Deflection of Marine Propellers
by J. P. Sikora

28 Lasers for Hydrographic Applications
by M. B. White

DEPARTMENTS

19 Profiles in Science

39 Research Notes

About Our Cover

Computed diagrams, like those on this issue's cover, are helping to predict ship hydrodynamic performance. See page 3.

Naval Research Reviews publishes articles about research conducted by the laboratories and contractors of the Office of Naval Research and describes important naval experimental activities. Manuscripts submitted for publications, correspondence concerning prospective articles, and changes of address, should be directed to Code 733, Office of Naval Research, Arlington, Va. 22217. Requests for subscription should be directed to the Superintendent of Documents, U.S. Government Printing Office, Washignton, D.C. 20402. Yearly subscription prices for this quarterly publication are $6.50 in the United States and Canada and $8.15 elsewhere. The issuance of this periodical is approved in accordance with Department of the Navy publications and printing regulations.

Rear Admiral Leland S. Kollmorgen, USN, was confirmed by Congress and assumed the duties as Chief of Naval Research on July 24. He will also serve in the additional duty capacity as Deputy Chief of Naval Material (Technology) and Chief of Naval Development. He heads the Office of Naval Research and the Office of Naval Technology.

In these capacities, he directs the planning and execution of the Department of the Navy Technology Base (basic research and exploratory development) programs. In addition, he is responsible for the administration and supervision of all Department of the Navy activities relating to patents, inventions, trademarks and copyrights. As Chief of Naval Research, Admiral Kollmorgen exercises management and technical control of the Naval Research Laboratory in Washington, D.C.; the Naval Ocean Research and Development Activity in Bay St. Louis, Mississippi; the Naval Biosciences Laboratory in Oakland, California; and Branch Offices in the United States and overseas.

A native of Los Angeles, California, Admiral Kollmorgen enlisted in the Navy in 1945 and received a fleet appointment to the U.S. Naval Academy in 1947. Upon graduation he was assigned to the USS KIMBERLY as Communications Officer in 1951. During this tour, he saw service with the 7th Fleet in Korean waters.

Following designation as a Naval aviator in 1954, Admiral Kollmorgen served tours with Attack Squadron 115, Heavy Attack Squadron Four, and Heavy Photographic Squadron 61. In 1967, he reported to Attack Squadron 161 as Executive Officer and then Commanding Officer the following year. In 1970 Admiral Kollmorgen assumed command of Attack Squadron 128, the A-6 Replacement Training Squadron, with additional duty as Medium Attack Wing Commander for Commander Fleet Air, Whidby Island, Washington. His subsequent tours of duty have been on the staff of the Deputy Chief of Naval Operations for Air Warfare; Special Assistant to the Director, Navy Program Planning; Command of the Naval Air Station, Cecil Field; Military Assistant to the President; Assistant Director, Strategic and Support Systems, Test and Evaluation, in the Office of the Director, Defense Research and Engineering. His last assignment before coming to ONR was Director, Systems Analysis Division, Office of the Chief of Naval Operations.

Rear Admiral Kollmorgen, USN– New Chief of Naval Research

Five Years of Numerical Naval Ship Hydrodynamics at DTNSRDC *

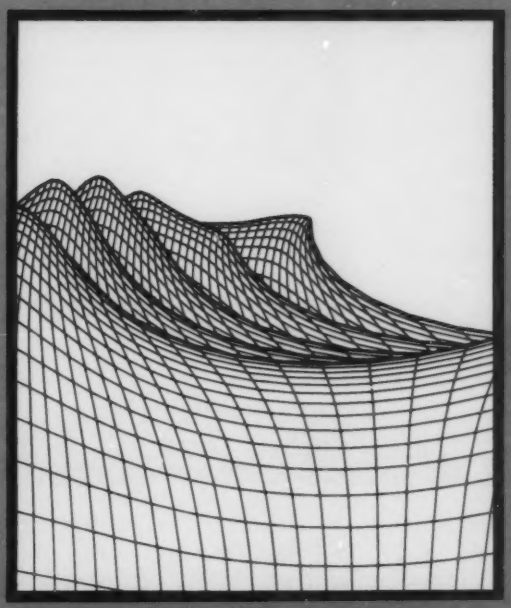

Computed breaking wave development.

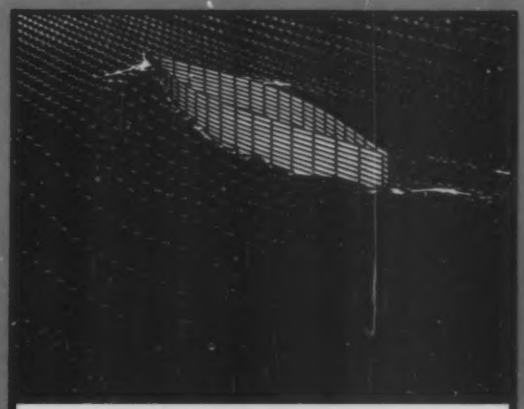

Above: Computed ship generating waves
Below: Transom stern generating waves

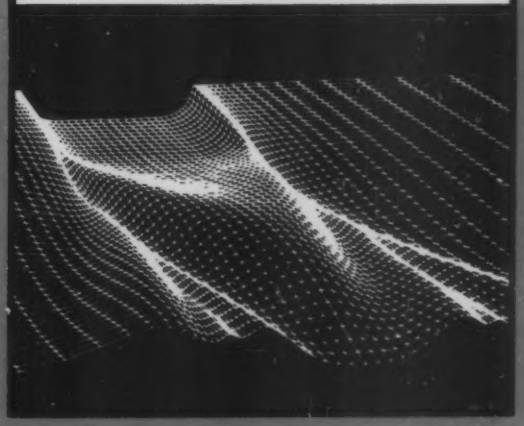

by

Nils Salvesen **
David W. Taylor
Naval Ship Research
and Development Center

Introduction

Over the last two decades, there have been impressive advances in the development of computational methods for predicting ship-hydrodynamic performance characteristics. Many of these computational tools are now being used routinely in the design of new naval ships and in improving the hydrodynamic performance of existing ships. However, these existing tools have some severe limitations because they are based on theories in which drastic approximations have been applied in order to reduce the computational effort. New computational methods with superior accuracy are needed to solve many of today's challenging ship-design problems. It is believed that many of the ship-hydrodynamic problems can be solved more effectively by applying advanced numerical methods rather than by traditional analytical methods. Numerical methods are defined as methods which rely heavily on large-scale numerical

**This is an abbreviation of a paper to be published in the Journal of Ship Research (1981).*

***Presently with Science Applications, Inc., Annapolis, Maryland.*

computations where the governing differential equations and boundary conditions or governing integral equations may be solved directly, for example, by finite difference, finite element, spectral, or panel methods.

The Navy recognized the demand for advanced numerical methods to predict the hydrodynamic performance characteristics of naval ships and in July 1974 the Numerical Naval Ship Hydrodynamics Program was established at the David W. Taylor Naval Ship Research and Development Center (DTNSRDC). The objective of the program is to develop new numerical methods to evaluate hydrodynamic performance characteristics that cannot be satisfactorily predicted by traditional methods. The program has been jointly supported by the Office of Naval Research, the Naval Sea Systems Command, and DTNSRDC through its Independent Research Program. In this article, we will review the research activity and progress in the first five years of this program (through July 1979).

The effort in numerical naval ship hydrodynamics during this period was devoted to the reexamination of inviscid free-surface problems, such as the problems of ship wave resistance and ship motions in waves. These free-surface problems have a long history of development using classical analysis which eschews substantial computational efforts and relies on simplifying ship-hull boundary conditions and linearized free-surface conditions. These classical methods have resulted in several useful computer codes which are in use today for predicting certain ship-hydrodynamic performance characteristics. However, the classical computational methods have some severe limitations that greatly restrict their application to naval ship design. For example, the strip theory of ship motions which has been in use for several years, is inaccurate at high ship speeds. The conventional methods used for predicting wave resistance cannot be applied for predicting the flow in the immediate neighborhood of the ship hull or for predicting the wave resistance of high-speed naval ships with transom sterns. In the next section, we will present the accomplishments of the Program and will discuss several new numerical methods that have accuracy superior to the classical computational methods.

The DTNSRDC has played a major role in fostering an international community in numerical ship hydrodynamics. The First Numerical Ship Hydrodynamics Conference held in Gaithersburg, Maryland. in October 1975 was initiated and organized by the DTNSRDC and the Second Numerical Ship Hydrodynamics Conference held in Berkeley, Calif. in September 1977 was jointly organized by the University of California and the DTNSRDC. Furthermore, the DTNSRDC organized and hosted an international Workshop on Ship Wave Resistance Computations in November 1979. The purpose of the Workshop was to evaluate existing computational methods for predicting the wave resistance and local flow field of ships.

The initial phase of the program has been very effective. It has resulted in a significant advance of the state-of-the-art of the prediction of ship hydrodynamics. Also, it has demonstrated that numerical approaches can have superior advantages over the more traditional methods in solving certain classes of ship hydrodynamics problems. The initial phase of the program can now be considered largely complete. The program should now expand its effort and include other problem areas in naval ship hydrodynamics where it can be expected that the development of advanced numerical methods for the solution of these problems will succeed and where it has been shown that pure analysis and simplified calculations have failed to give adequate solutions.

Accomplishments

The limitations and inaccuracies of the classical methods, for the ship-wave problems chosen during the initial phase of the Numerical Program, are mainly due to four major assumptions. Therefore, the first aim of the Numerical Program has been to systematically remove or improve at least some of these four critical assumptions:

- **Small viscous/wave interactions.** The interactions between the viscous effects and the gravity waves are assumed to be small so that potential-flow theory can be used in predicting, for example, ship motions and wave resistance.
- **Linearization of free-surface conditions.** It is assumed that the wave slopes of the incoming and the ship-generated waves are sufficiently small so that the nonlinear free-surface boundary conditions can be replaced by the linearized conditions.
- **Hull-form approximation.** The exact hull boundary condition is replaced by some approximate condition and the theories are usually categorized accordingly. Examples are thin-ship theory, strip theory, and slender-body theory.
- **Small amplitude ship motions.** For ship motion problems, it is assumed that the unsteady body displacements are small so that the hull boundary condition can be satisfied at the mean position of the ship.

Prior to the start of the Numerical Program, practically all of the classical methods which were used for predicting the ship hydrodynamic performance characteristics were based on these assumptions. The effort of the initial phase of the Numerical Program has been concentrated on the improvement or removal of the last three assumptions.

Linear Ship-Wave Solutions

It was decided that in developing the first generation of numerical methods for solving three-dimensional ship-wave problems, the first two assumptions cited above should be applied. In other words, potential-flow theory with linearized free-surface condition should be applied initially. The effort should be concentrated on improving or removing the last two assumptions applied to the hull boundary condition.

This decision was made not because viscous interaction effects or non-linear free-surface effects are less important than the correct satisfaction of the hull boundary condition, but because it is much easier to improve the latter. Furthermore, by satisfying the exact hull-boundary condition, the local flow field can be computed with much better accuracy than by, for example, the conventional thin-ship theory. (Thin-ship theory assumes that the beam is much smaller than the draft and the length.) Accurate predictions of the local flow field are important in solving many important naval ship design problems, as, for example, bow cavitation, flow separation, and inlet/outlet flows. Accurate information about the local flow field is also a required input to existing computer codes for predicting three-dimensional viscous boundary layers.

Wave Resistance and Local Flow

The first problem which we shall consider is prediction of the wave resistance and the local flow field of a ship advancing at constant forward speed in calm water. Our initial objective has been to develop computational methods which satisfy the exact hull boundary condition and the linearized free-surface condition in an ideal fluid. There is good reason to believe that such an approach will yield accurate local-flow predictions over most of the hull and also improved wave-resistance predictions. Four different numerical methods for predicting the wave resistance and the local flow field of a ship advancing in calm water have been developed, all of which satisfy the exact hull boundary condition:

Dr. Salvesen is a naval architect on the staff of Science Applications Incorporated, Annapolis, MD. He is internationally recognized as an expert in nonlinear ship-wave theory and on the theoretical and computational methods for predicting motions and wave-induced loads on ships and floating platforms. While at DTNSRDC he was the initiator and leader of the Numerical Naval-Ship Hydrodynamics Program.

1. The double-model linearization method (Dawson, 1977).
2. The Green's function method (Chang, 1977).
3. The finite-element method (Bai, 1977).
4. The fast direct matrix solver method (Ohring and Telste, 1977).

In Dawson's double-model linearization method, the free-surface boundary condition is linearized with respect to the double-model velocity potential. The solution is generated by a source-density distribution on the body surface and on the local part of the undisturbed free surface.

The streamlines along the hull surface of a typical high-speed cargo ship computed by the Dawson numerical method are shown in Figure 1. The upper part of the figure shows the streamlines for the hull advancing in the free surface at Froude number*, $F_n = 0.35$, (corresponds to 26 knots for a 500-foot ship) and the lower part shows the streamlines for the double-model infinite-flow case. The solid lines numbered 1 through 7 are the computed streamlines, the

**Froude number is a nondimensional speed defined as $F_n = V/\sqrt{Lg}$ where V is ship speed, L is ship length, and g is the acceleration of gravity.*

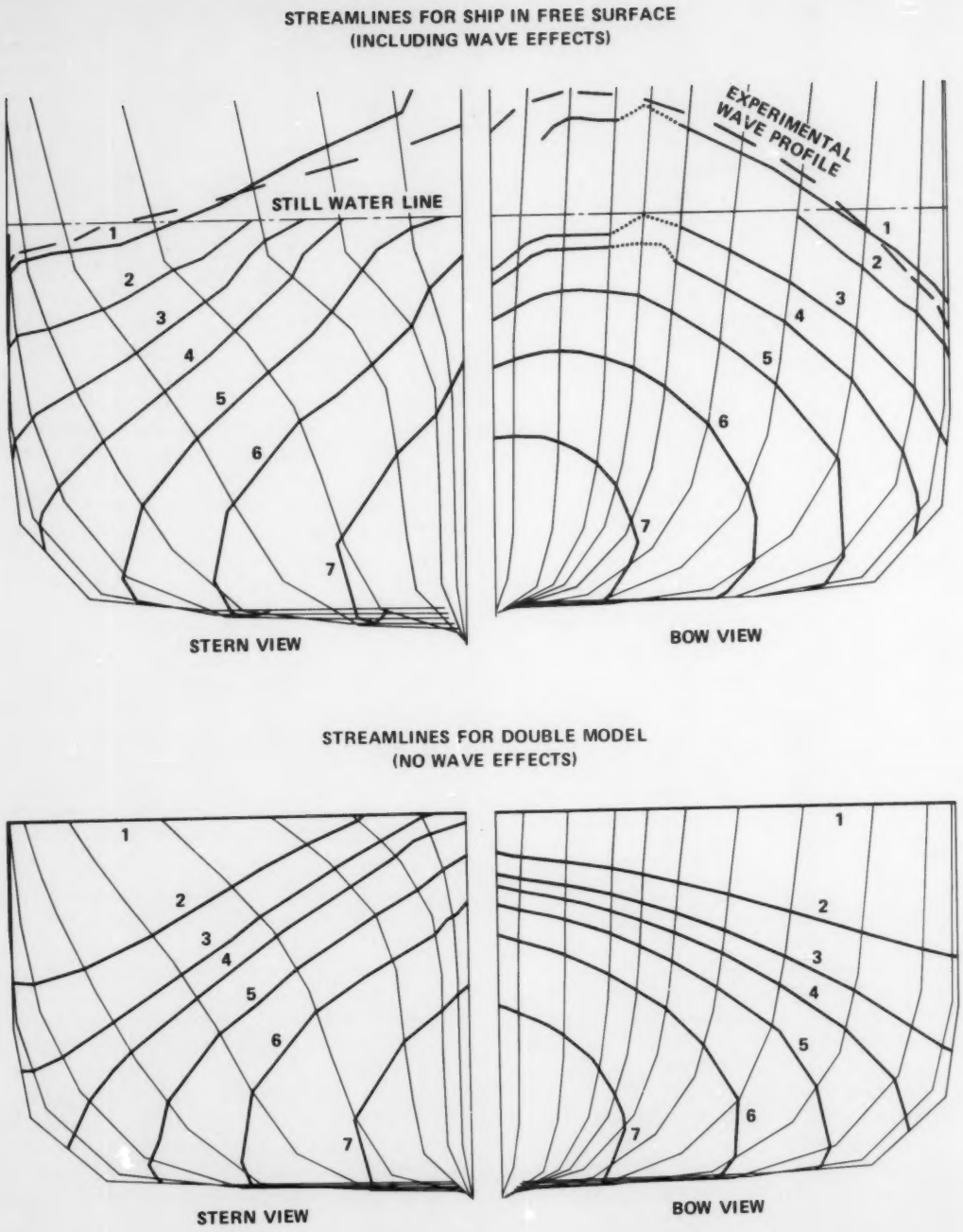

Figure 1. Streamlines on Hull Surface of a typical high-speed cargo ship at F_n = 0.35 (Dawson, unpublished)

uppermost streamline numbered 1 being the wave profile along the hull. The broken line is the experimentally measured wave profile. There is a considerable difference in the streamline trajectories between the free-surface case and the double model case. It clearly indicates that free-surface effects are important for accurate predictions of local flow at hull locations higher than about one-half of the ship's draft. The accuracy of these streamlines has not been completely evaluated, but preliminary analysis indicates that they are reasonable. Thus, it seems as if Dawson's computational method allows one to trace, apparently for the first time, reasonably accurate streamlines on surface ships.

The Green's function method of Chang (1977) which predicts the wave resistance and local flow about a ship is somewhat more traditional and makes use of more analytical results. In this method, the free-surface condition is linearized about the uniform stream velocity and the body-boundary condition is satisfied exactly by a distribution of Kelvin wave sources on the wetted surface of the hull. Again the resulting integral equation is solved by the panel method. It is believed that Chang's and Dawson's methods would give practically the same results at high ship speeds, whereas there may be some noticeable differences at low speeds.

The methods of Chang and Dawson first determine the trim and sinkage of the ship and then solve the flow problem for the actual trim and sinkage condition. Furthermore, in both these methods, the transom-stern* body-boundary condition is modeled accurately. These are all important factors in predicting the wave resistance of high-speed transom-stern ships ($F_n > 0.35$). Since these factors are not considered accurately by the existing classical methods, and since most naval ships are high-speed ships with transom sterns, it is expected that Chang's method and Dawson's method will be useful for many naval-ship applications. Results presented by Dawson and by Chang at the Workshop on Ship Wave Resistance Computations at DTNSRDC (1979) demonstrated that both methods have the potentials to predict accurately the wave-resistance of high-speed naval ships with transom sterns.

The next two methods for treating the wave-resistance problem make a clear break with the past and solve the partial differential field equation by numerical methods. Bai (1977) developed a localized finite-element method for the flow past a ship in a canal or towing tank. In this method, finite-element computations are only performed in a localized domain surrounding the ship, the domain D_0 in Figure 2a. In the other domains, D_1 and D_2 in Figure 2a, the velocity potential is represented by a finite sum of eigenfunctions (or Green's functions).

A typical wave resistance obtained by Bai's method is shown in Figure 2b. Bai's finite-element method has been used in this example to investigate blockage effects due to the finite dimensions of ship-model tanks (Bai, 1979). A very significant result has been found; namely, that the main difference in the total resistance coefficient measured at high values of Froude number in a large and a small towing tank is primarily due to the difference in the wave resistances computed for the two tanks. As a result of this finding, a new mean-speed correction formula due to blockage has been proposed.

The fourth method for solving the wave-resistance problem (Ohring and Telste, 1977) treats the time dependent problem in which, for example, a

Transom stern is a square-ended stern used to provide additional hull volume and deck space aft and to decrease resistance for high-speed ships.

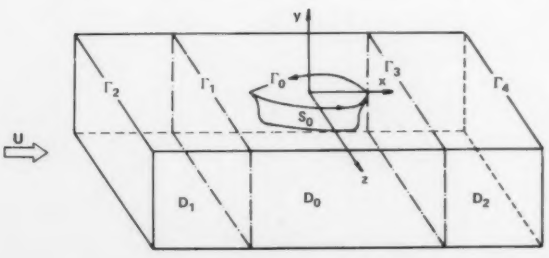

Figure 2a. The Three Subdivided Fluid Domains for the Localized Finite-Element Method

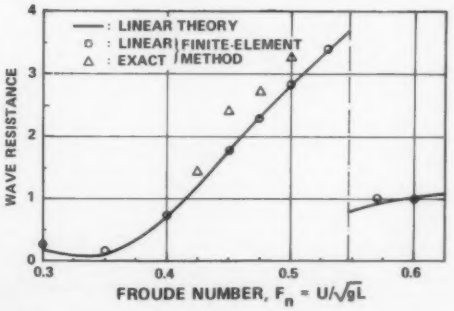

Figure 2b. Wave Resistance of a Wigley Parabolic Ship in a Canal

Figure 2. Wave Resistance Computed by Localized Finite-Element Method (Bai, 1977)

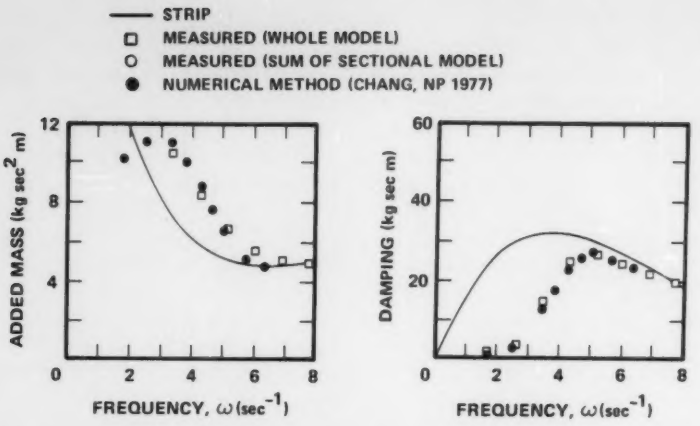

Figure 3. Pitch Added-Mass and Damping Coefficients for Series 60 Model, $C_B = 0.70$ at $F_n = 0$ (Chang, 1977)

ship may be accelerating from rest to some given steady speed. This method will be discussed in a separate section on Transient Ship-Wave Solutions.

Small Amplitude Ship Motions

Computer programs which are based on the conventional strip theory of ship motions have been used the last decade for predicting the motion and sea loads of naval ships. In the strip theory, the three-dimensional ship hydrodynamics problem is replaced by a summation of two-dimensional sectional problems and the forward-speed effects are only satisfied approximately. The strip-theory approach gives good results for heave, pitch, and roll motions in moderate seas and moderate ship speeds for most conventional hull forms; however, the method gives inadequate results for low frequencies, higher ship speeds and local pressure distributions. The forward speed limitation is the most severe restriction for naval applications.

Chang (1977) has developed a three-dimensional numerical method for predicting ship motions that solves the complete three-dimensional hydrodynamics problem and satisfies correctly all forward speed effects. The hydrodynamic problem is solved by dis-

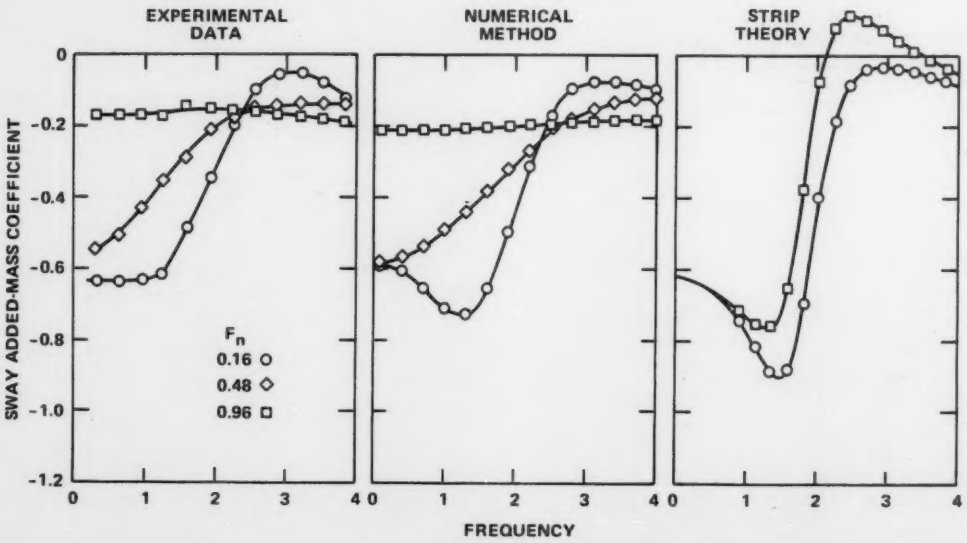

Figure 4. Flat Plate Sway Added-Mass Coefficients (Chapman, 1975)

tributing three-dimensional oscillating Kelvin sources (which satisfy the linearized free-surface boundary condition) on the undisturbed wetted hull surface. The strength of these singularities is obtained by solving the hull boundary condition. Some preliminary computations of added-mass* and damping coefficients obtained by Chang's three-dimensional method are shown in Figure 3. The added-mass and damping coefficients, next to the exciting forces are the most important hydrodynamic ingredients needed in predicting ship motions and wave induced loads. Figure 3 shows the added-mass and damping coefficients for pitch motions as a function of frequency of encounter for a conventional cargo ship (Series 60 model with back coefficient $C_B = 0.70$) at zero forward speed. Results obtained experimentally, by strip theory and by Chang's method are presented in the figure. It can be seen that Chang's three-dimensional numerical method agrees well with the experimental results throughout the frequency range, whereas the strip-theory results only agree well with the experimental values in the high-frequency range. These and similar results seem to indicate that Chang's method can predict the hydrodynamic coefficients used in predicting ship motions with better accuracy than the strip theory.

Another advance in the area of ship motions has resulted from Chapman's (1975) numerical work. He has shown that by applying slender-body theory,** the three-dimensional problem of a ship oscillating in the lateral model of motion (sway and yaw) can be reduced to a series of transient unsteady two-dimensional flow problems in the transverse plane. He developed a finite-difference numerical method for solving the resulting unsteady two-dimensional free-surface flow problem in the cross-flow plane. To evaluate the method, Chapman applied it to a flat plate for which experimental and strip-theory results were available. Figure 4 shows the sway added-mass coefficient as a function of frequency of oscillation for three Froude numbers, $F_n = 0.15$, 0.43, and 0.96. It can be seen that the results of Chapman's numerical method agree reasonably well with experiments, whereas those of the conventional strip theory do not.

Most computational methods for predicting the free-surface hydrodynamics of air-cushion vehicles (ACV) treat only the case of a constant pressure distribution moving over the water. However, the ambient wave field and resulting vehicle motions cause the cushion pressure of an ACV to vary with time. Therefore, Haussling and Van Eseltine (1978) developed a new method for computing the three-dimensional flow for a moving time-dependent pressure distribution. This method exploits another numerical technique in which Fourier series are used to represent the flow field. Haussling and Van Eseltine have found that this method may be applied successfully to a large variety of unsteady free-surface pressure problems. For the two-dimensional case, it has been shown analytically that there exists a critical combination of cushion oscillation frequency and forward speed for which the resistance becomes infinite. Haussling and Van Eseltine showed numerically that, for the three-dimensional case, waves in front of the disturbance are generated at similar critical combinations of frequency and forward speed; however, the wave resistance remains finite. Figure 5a shows the computed waves generated by a rectangular pressure distribution advancing in calm water with the pressure oscillating at the critical frequency for this particular speed, $F_n = 0.40$. In this figure one clearly can see the computed waves in front of the disturbance (the top part of the picture) generated at this critical frequency. Figure 5b shows the computed in-phase resistance as a function of the frequency of the pressure oscillations for three forward speed cases (Froude number, $F_n = 0.4$, 0.5, and 1.0). It can be seen in Figure 5b that at the critical frequency depicted in Figure 5a ($\omega = 0.625$ and $F_n = 0.40$) the resistance is large but finite. An important part of the finding of Haussling and Van Eseltine is that the increased resistance at the critical frequency diminishes with increasing Froude numbers. Therefore, for high-speed ACV, this critical frequency problem is not as important as may have been believed previously.

Transient Ship-Wave Solutions

Prior to the start of the Numerical Program no computational methods existed for predicting the free-surface flow about a ship undergoing unsteady forward motions. The computer codes existing prior to 1974 for solving ship-wave problems were restricted to cases where the ship has constant speed and/or harmonic motions. Recently, a numerical finite-difference scheme was developed by Ohring (1975) which solves the hydrodynamic problem of a ship accelerating along a straight path in a channel of calm water. A fast direct matrix solver has been used by Ohring to reduce the computational time involved in solving the Laplace equation at each grid point at

Added mass is the additional mass due to the presence of the water.

***Slender-body* theory assumes that both the beam and the draft are much smaller than the length.*

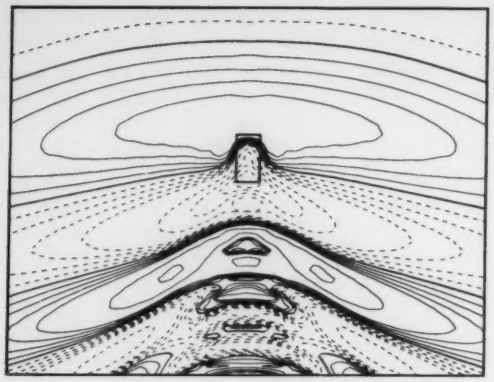

Figure 5a. Oscillating Pressure Disturbance Advancing at Froude Number, F_n = 0.40

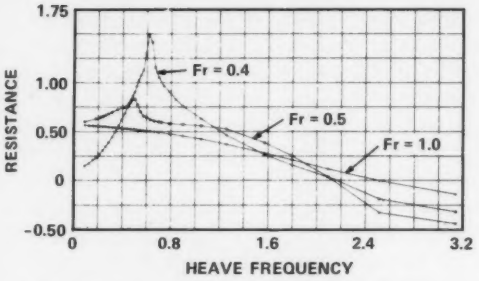

Figure 5b. Resistance for Three Froude Numbers

Figure 5. In-Phase Wave Elevations and Resistance for Oscillating Pressure Distribution (Haussling and Van Eseltine, 1978)

each time interval. In Ohring's method the body boundary condition is satisfied at the exact body location, and the free-surface condition is linearized.

Typical results using Ohring's method for a surface effect ship (SES) accelerating abruptly from rest to a constant speed are presented in Figure 6.

The SES is represented by a pressure distribution between two thin plates. This result seems to indicate that the flow is nearly two-dimensional between the two plates and that three-dimensional effects dominate the free-surface disturbance only behind the body. These results demonstrate the potentials of these new numerical methods in obtaining solutions of hydrodynamic problems which were beyond the capability of conventional methods of analysis.

Ship Maneuvering

At the present time, ship maneuvering characteristics cannot be predicted by any purely computational method. The time-domain computer simulation methods now in use at the DTNSRDC for estimating ship maneuvering characteristics utilize several experimentally obtained coefficients. Therefore, one objective of the Numerical Program has been to develop not only purely computational methods for predicting ship maneuvering characteristics, but also to develop numerical methods for predicting the hydrodynamic coefficients needed for the time-domain simulation of ship maneuvering.

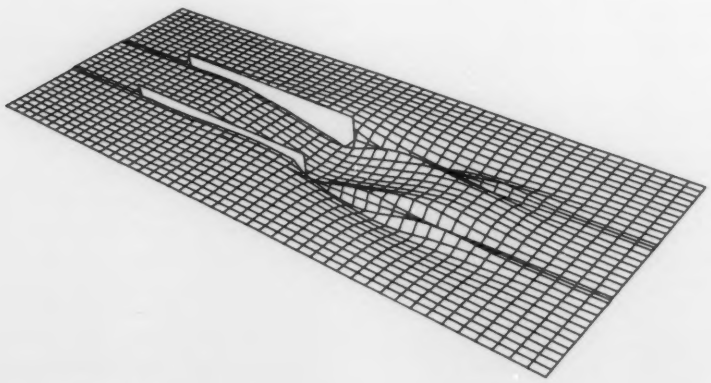

Figure 6. Free-Surface Elevations for Accelerating Surface Effect Ship (Unpublished)

Haussling and Van Eseltine (1976a) have developed a method for analyzing the local flow field and the hydrodynamic forces and moments on an air-cushion vehicle (ACV) performing any prescribed maneuver in calm water or in some given sea condition. In this method, the ACV is represented by a specified pressure distribution which may be a function of time. The potential flow problem is solved in a completely confined fluid domain so that Fourier series representation of the potential can be used. The final results include the wave resistance, side force, yawing moment, total power, wave elevations, and local flow field.

Sample results obtained by the method of Haussling and Van Eseltine are presented in Figures 7 and 8. Figure 7 shows the wave contours for an ACV performing a turn in otherwise calm water, whereas Figure 8 shows the yawing moment exerted on the ACV and the power expended by the ACV as functions of time for the case of an ACV moving over a disturbed sea. It is anticipated that this numerical method will have many useful applications since it treats the very general case of an ACV moving with arbitrary trajectories in a specified sea condition.

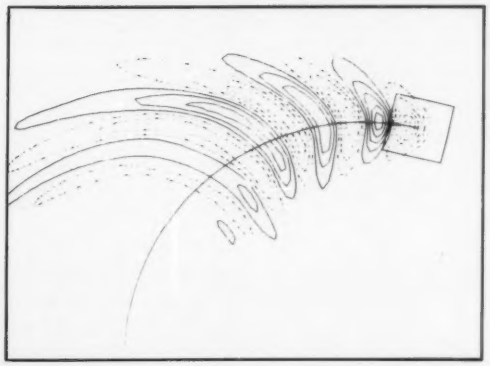

Figure 7. Wave Elevations Generated by an Air Cushion Vehicle Moving over Calm Water (Haussling and Van Eseltine, 1976a)

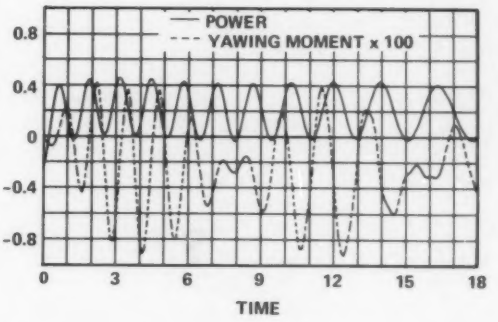

Figure 8. Yawing Moment and Power versus Time for an Air Cushion Vehicle Moving over a Disturbed Sea (Haussling and Van Eseltine, 1976a)

The lateral stability characteristics of a body depend primarily on its outline, so that a vertical flat plate is a useful model of a maneuvering monohull, strut, or surface effect ship. For this reason Chapman (1976) has developed a method for predicting the flow past vertical yawed surface piercing plates advancing at constant speed. Figure 9 shows the computed free-surface disturbance generated by a yawed plate. The three-dimensional problem is solved by applying slender-body approximations and solving the resulting two-dimensional initial-value problem by a finite-difference method. Chapman (1976) developed separate numerical methods for linear, second-order, and nonlinear free-surface conditions. Results for the side-force coefficient are shown in Figure 10 where, in the upper right corner, the grid system for the nonlinear method is shown.

Large-Amplitude Ship Motions

In linear ship-motion theories, it is assumed not only that the free-surface conditions can be linearized, but also that the ship displacements are small relative to the ship dimensions. The exact body-boundary condition then can be approximated by satisfying it at the mean position of the hull. However, ship motions cannot always be assumed to be small. In fact, they can be on the order of magnitude of the ship dimensions even in typically moderate sea conditions.

Figure 11 shows computed bow motions of a destroyer hull in head waves (Salvesen, 1978). These results indicate that the bow displacement is nearly equal to the ship draft for waves with a height-to-length ratio H/λ of only 0.013. Since the maximum value of H/λ for nonbreaking waves is almost ten times this value (Salvesen and von Kerczek, 1976), one may expect that the assumption of small bow displacements is violated during a large portion of the ship's operating life.

Therefore, another goal of the Numerical Program is to develop new numerical methods which can predict large amplitude ship motions. This is a very complicated nonlinear problem where linearization

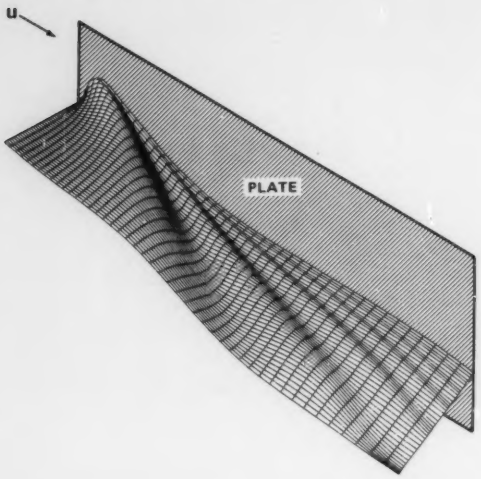

Figure 9. View of Free Surface for Plate Yawed to Starboard (Chapman, 1976)

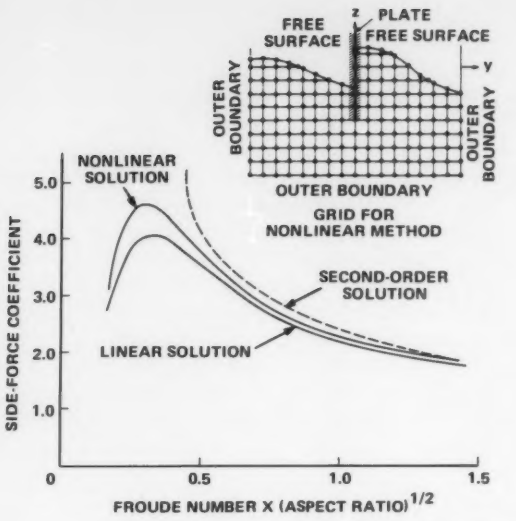

Figure 10. Linear, Second-Order, and Nonlinear Solutions for Side-Force Coefficients for Yawed Plate (Chapman, 1976)

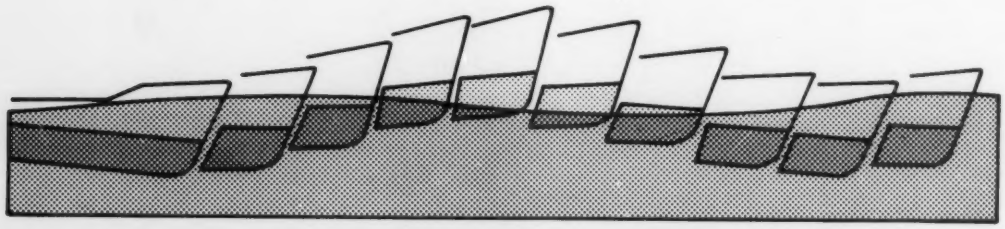

Figure 11. Bow Motion of Destroyer Hull in Sinusoidal Wave with Wavelength, $\lambda = 1.20L$, Wave Height, $H/\lambda = 0.013$, and Froude Number, $F_n = 0.35$ (Salvesen, 1978)

cannot, in general, be applied to the boundary conditions at the hull or at the free surface. However, if it is assumed that the frequency of the ship motions is sufficiently small,* and that the slope of the incident waves is fairly small, then it may be valid to linearize the free-surface conditions even for large body displacements.

As a start on developing such a low-frequency ship-motion theory, Chapman (1979) has developed a two-dimensional, large-amplitude, time-domain method with a linearized free-surface condition. A spectral representation of the wave field combined with a source distribution over the entire body, as shown in Figure 12, is used. There are no restrictions with regard to the body displacement other than that the motions must be so slow that they only result in small free-surface disturbances. For example, the upper part of the body (the deck) may become completely submerged. An application of this method is the analysis of capsizing problems. Figure 13 shows results computed by Chapman for the wedge-entry problem. The free-surface elevations at three time steps are shown for a wedge with half angle, $\psi = 15$ degrees.

**Note that when the frequency is small, the slope of the body-generated waves will also be small.*

Nonlinear Two-Dimensional Solutions

A major difficulty in solving ship-wave problems is that the free-surface boundary conditions are not only nonlinear, but they must be satisfied at the actual location of the free surface which is ***a priori***

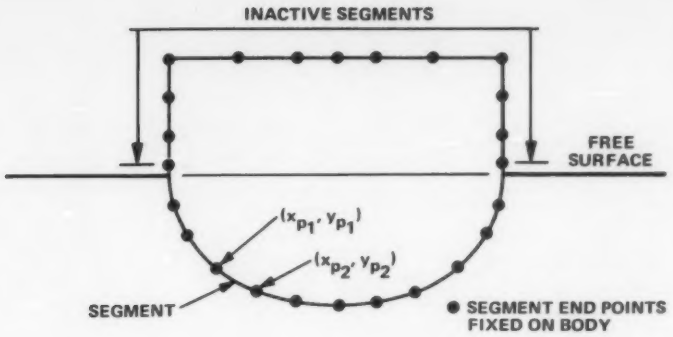

Figure 12. Body Segments for Large-Amplitude Body-Displacement Computations (Chapman, 1979)

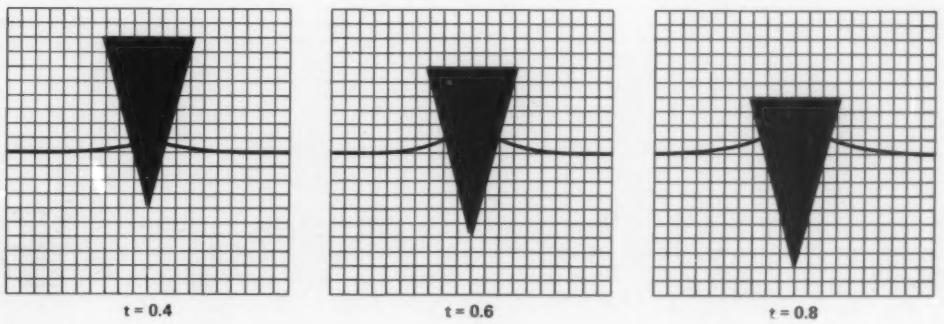

Figure 13. Free-Surface Elevations for Wedge Entry, Half-Angle, $\psi = 15°$ (Chapman, 1979)

unknown and must be found as part of the solution. Classical analytical techniques attempt to overcome this problem by building up perturbation solutions about a known free surface (the uniform stream).

Part of the effort in the Numerical Program was devoted to research on numerical methods in which the nonlinear implicit equations are solved directly. Because this was considered to be an immense task for three-dimensional problems, initial efforts were confined to two-dimensional nonlinear free-surface problems. It is hoped that the experience gained from the two-dimensional problems would provide a guide to the solution of the three-dimensional problems.

Steady Body-Wave Problems

The steady nonlinear problem of uniform flow past a disturbance may be solved by two approaches: (1) it may be solved in the time domain as an initial-value problem advancing toward steady-state conditions, and (2) it may be solved as a steady-state problem in which an assumed free-surface shape is iterated until the free-surface conditions are satisfied. In this section we shall discuss first the steady-state iteration approach. The initial-value approach will be discussed in the next section on unsteady problems.

A numerical method has been developed which solves the exact nonlinear potential-flow problem for two-dimensional hydrofoils, and free-surface pressure distributions advancing at uniform speed in otherwise undisturbed water of finite depth. The Laplace equation is approximated by a five-point

finite difference equation in a field bounded by an assumed free-surface shape which is systematically corrected until the free-surface conditions are satisfied. Von Kerczek and Salvesen (1974) demonstrated that this iteration scheme converges to a steady solution with periodic waves downstream of the disturbance. The finite difference grid system and the location of the submerged vortex, which was used to simulate a hydrofoil in this case, is schematically shown in Figure 14.

Von Kerczek and Salvesen have used this finite-difference method in the investigation of several important nonlinear aspects of free-surface flow past two-dimensional disturbances. They have demonstrated that the method can solve problems which are highly nonlinear and with wave steepnesses near that for which waves are observed to break. For most of the cases investigated, they have found good agreement between the numerical results obtained by solving the complete nonlinear problem and third-order perturbation theory results. Furthermore, these investigations have shown that for subcritical shallow-water flow some of the nonlinear free-surface effects are very sensitive to depth. In the following paragraphs some sample results obtained by von Kerczek and Salvesen will be discussed.

Figure 15 shows the wave resistance as a function of vortex circulation predicted both by the numerical finite-difference method and by first-, second-, and third-order perturbation theory (Salvesen and von Kerczek, 1976). The agreement between third-order theory and numerical results is remarkable even for the larger vortex strengths where the steepnesses of the generated waves are close to the breaking limit.

Salvesen and von Kerczek (1975) have demonstrated that their numerical iteration method predicts with good accuracy the wave resistance and the waves generated by a hydrofoil moving at a fixed submergence with uniform speed. Figure 16 shows the shape

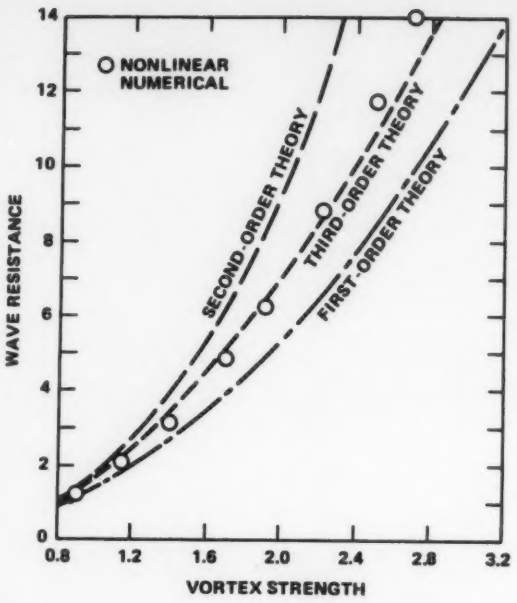

Figure 15. Wave Resistance as a Function of the Strength of Submerged Vortex Advancing at Constant Speed (Salvesen and von Kerczek, 1976)

of the foil that was used as a test case and the finite-difference grid system that was used in their calculations. A series of experiments in a towing tank was conducted with this hydrofoil and Figure 17 shows a photograph of one test result. The free-surface elevations predicted by linear theory and the numerical method, and those obtained experimentally are compared in Figure 18. It is seen that the numerical results obtained by solving the complete nonlinear problem agree well with the experimental results whereas there are larger discrepancies between the linear theory predictions and the experimental re-

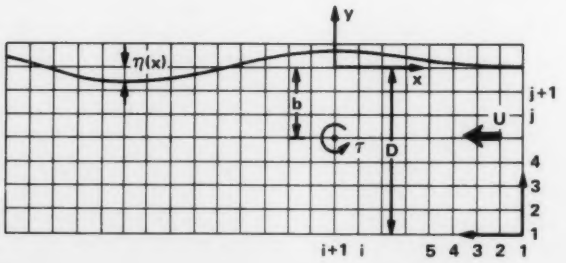

Figure 14. Finite Difference Grid for Submerged Vortex Case (Salvesen and von Kerczek, 1976)

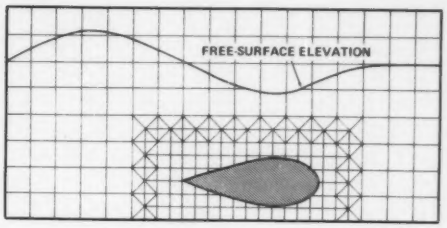

Figure 16. Finite Difference Grid System for Submerged Foil (Salvesen and von Kerczek, 1975)

Figure 17. Experiment for Foil Advancing at U = 3.3 ft/sec (Salvesen and von Kerczek, 1975)

sults. Linear theory underpredicts the wave amplitudes and overpredicts the wavelengths.

Probably one of the most important findings of the above cited studies of two-dimensional nonlinear waves generated by a traveling obstacle is the fact that third-order perturbation theory agrees well with numerical results even for waves whose steepness is close to that at which wave breaking is observed. This is very encouraging because it indicates that a perturbation theory may also predict accurately the nonlinear aspects of the complete three-dimensional ship-wave problem. Perturbation methods have many advantages over completely numerical schemes which satisfy the exact free-surface boundary conditions. One advantage is the much shorter computation time, but probably more important is the fact that all of the numerical methods, including the unsteady methods we shall discuss in the next section, have severe difficulties with numerical convergence in the case of very steep waves. We feel, therefore, that a third-order perturbation approach may ultimately be a useful practical solution method for the nonlinear ship-wave problem.

Unsteady Body-Wave Problems

A considerable effort has been concentrated on numerical solutions of the initial-value problem of a two-dimensional body starting from rest with arbitrary motion. Ideal fluid is assumed and the exact free-surface conditions are satisfied. In the initial-

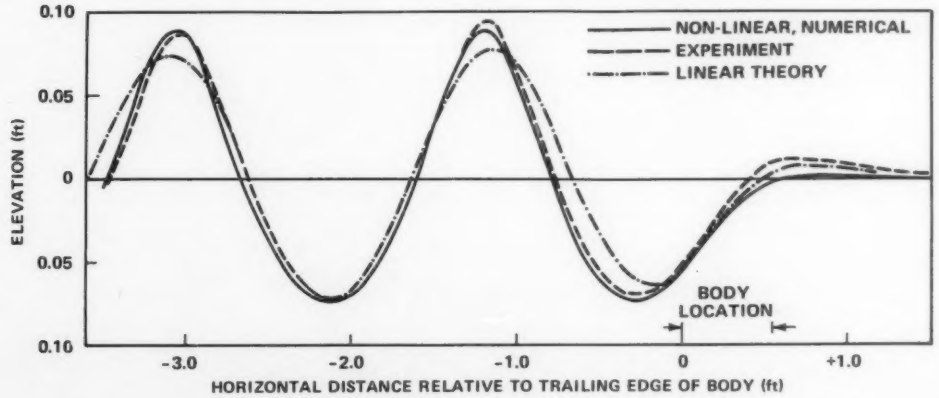

Figure 18. Comparison of Experimental, Theoretical, and Numerical Free-Surface Elevations for Submerged Foil Advancing at U = 3.18 ft/sec (Salvesen and von Kerczek, 1975)

value unsteady problem method one can obtain solutions for both the transient phase of the body motion and the steady phase by letting the time advance to appropriate values. Haussling, Van Eseltine, and Coleman have developed some efficient numerical methods for solving several interesting unsteady nonlinear free-surface problems. We shall briefly discuss some of their encouraging results.

Haussling and Van Eseltine (1976b) have developed a finite-difference method for solving two-dimensional unsteady planing-body problems. An extension of this method (Haussling, 1979) has been used in a study of the nonlinear effects of two-dimensional stern waves as shown in Figure 19. From this study, Haussling concludes that "for draft-based Froude numbers (F_n) less than three, the nonlinear effects can be significant." Presently, a code for solving the three-dimensional transom-stern wave problem is being prepared. We expect that this study will reveal some of the unknown aspects of the flow past transom sterns. It is very important in solving the wave-resistance problem for high-speed transom-stern ships that the conditions at the trailing edge be satisfied accurately.

As already stated, the initial-value approach is a useful method for solving steady-state nonlinear ship-wave problems. However, most investigators using the initial-value approach have encountered difficulties in obtaining steady-state conditions with steep nonbreaking waves. Haussling and Coleman (1977) have obtained steady-state conditions with wave steepnesses approximately 80 percent of the steepness at which waves are observed to break. For steeper waves, their method encounters difficulties with regard to numerical stability at such an early time step that a wave train has not yet been developed behind the first wave crest aft of the body. Figure 20 shows the wave profile obtained by linear theory and the unsteady profile obtained by the nonlinear numerical method of Haussling and Coleman at the last time step before the computations broke down due to numerical instability. Haussling and Coleman state that after this time step, "features develop which cannot be adequately handled by the numerical scheme." Whether such features have anything to do with physical reality has not yet been determined and requires much experimental and numerical study.

One of the critical problems with the unsteady approach is that even if a steady-state condition with nonbreaking waves exists, an unsteady numerical method may fail because of the presence of wave breaking during the transient period. Model-tank experiments have shown that there are steady-state conditions with stable nonbreaking waves that can only be obtained by accelerating the body through intermediate conditions where wave breaking is present.

Concluding Remarks

The research conducted under the Numerical Naval Ship Hydrodynamics Program has yielded numerical methods for solving several ship-wave problems that could not have been solved five years ago and cannot be solved today by the traditional nonnumerical methods. The problems for which we now have successful potential-flow solution methods can be grouped into five areas:

1. The ship-wave resistance and local flow problem with linearized free-surface conditions and exact

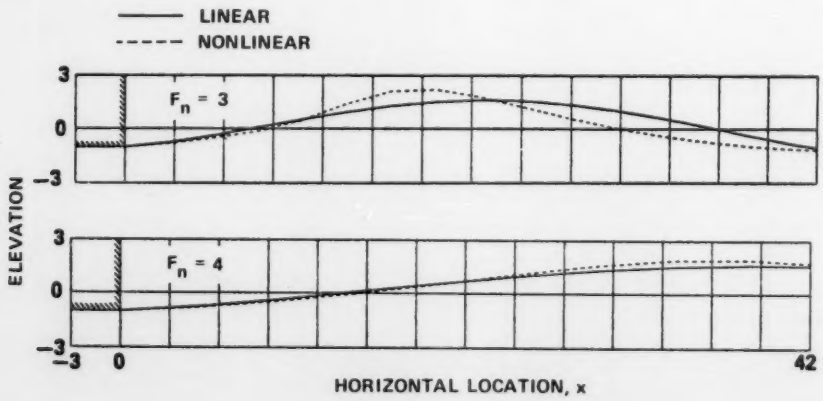

Figure 19. Linear and Nonlinear Waves behind a Transom Stern at F_n = 3 and F_n = 4 (Haussling, 1979)

body boundary conditions; Dawson (1977), Chang (1977), Bai (1977), Ohring and Telste (1977).

2. The fully three-dimensional ship motion problem with linearized free-surface conditions and the hull boundary condition satisfied at the mean position; Chang (1977).

3. The exact nonlinear two-dimensional steady-state body-wave problem; Salvesen and von Kerczek (1978).

4. The exact nonlinear two-dimensional unsteady body-wave problem for moderately steep waves; Haussling and Coleman (1979).

5. The large amplitude two-dimensional body motion problem with exact body boundary condition and linearized free-surface conditions; Chapman (1979).

Significant advances have also been made on several other important problems as discussed in the main text. However, only in the above stated areas can we consider that research is, in general, complete and further refinements and validation should be transferred to the development phase.

During the first five-year phase of the Numerical Program, the emphasis has been on ship-wave problems that can be solved by potential-flow theory. We believe that the research effort in this area should be continued and that the most important unsolved potential-flow ship-wave problems are:

1. The nonlinear three-dimensional ship-wave resistance and local flow problem.

2. The large amplitude ship-motion problem.

The experience gained from the nonlinear two-dimensional research seems to indicate that a useful and immediate solution method for the nonlinear wave-resistance problem may be obtained by a perturbation method. Methods should also be developed for analyzing cases with extreme nonlinear effects as, for example, wave breaking and spray. The energy dissipation due to such effects is an important aspect of the total resistance problem for most high-speed naval ships.

The Numerical Program should now expand its effort and include other problems in the following areas of ship hydrodynamics:

1. Ship wave making and viscous boundary layer interaction.

2. Ship boundary layers and large-scale separated flow, including vortex shedding.

3. Hydrodynamics of ship propulsion.

It is believed that the application of advanced numerical techniques and computers to these other important areas of naval hydrodynamics may be as rewarding as their application has been to ship-wave problems.

At the Berlin Towing Tank 75th Jubilee Conference in 1978, Marshall P. Tulin discussed the future role of the computer relative to model experiments with regard to the prediction of ship hydrodynamic performance characteristics. He asked several of the model tank directors the following question: "Which old (model tank) tasks will be taken over by computers?" The answer given by Dr. W. E. Cummins deserves some attention. He stated simply: "Most of them." It is not hard to agree with this view considering the technical accomplishments over the last couple of decades and what can be expected within the next one or two decades. However, we must be aware that Dr. Cummins' prediction about the future role of computers can only become a reality if adequate support is given to the implementation of the research results. The implementation is a challenging task in itself and has not been given sufficient attention in the past. ■

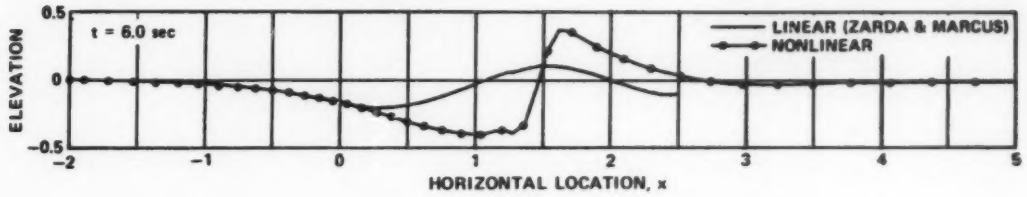

Figure 20. Nonlinear Unsteady Free-Surface Elevation for Translating Cylinder Compared with Linear Steady-State Results (Haussling and Coleman, 1977)

Acknowledgments

I wish to express my thanks to Justin H. McCarthy, Joanna W. Schot, Christian H. von Kerczek and Henry J. Haussling for their encouragement, advice, and assistance during the preparation of this report.

BIBLIOGRAPHY

All of these publications have been supported by the Numerical Naval Ship Hydrodynamics Program.

1. Bai, K. J., "A Localized Finite-Element Method for Steady, Three-Dimensional Ship-Wave Problems" (1977).**

2. Bai, K. J., "Blockage Correction with a Free Surface," Journal of Fluid Mechanics, Vol. 94, Part 3 (1979).

3. Chang, M. S., "Computations of Three-Dimensional Ship Motion with Forward Speed" (1977).**

4. Chapman, R. B., "Numerical Solution for Hydrodynamic Coefficients of a Surface-Piercing Strut" (1975).*

5. Chapman, R. B., "Free-Surface Effects of Yawed Surface-Piercing Plates," Journal of Ship Research, Vol. 20, No. 3 (1976).

6. Chapman, R. B., "Experimental Forces and Free-Surface Elevations for a Yawed Surface-Piercing Plate," DTNSRDC Report 77/0002 (1977).

7. Chapman, R. B., "Large Amplitude Transient Motion of Two-Dimensional Floating Bodies," Journal of Ship Research, Vol. 23, No. 1 (1979).

8. Dawson, C. W., "A Practical Computer Method for Solving Ship-Wave Problems" (1977).**

9. Haussling, H. J., "Two-Dimensional Linear and Nonlinear Stern Waves," Journal of Fluid Mechanics, (1979).

10. Haussling, H. J. and R. M. Coleman, "Finite-Difference Computations Using Boundary-Fitted Coordinate Systems for Free-Surface Potential Flows Generated by Submerged Bodies" (1977).**

11. Haussling, H. J. and R. M. Coleman, "Nonlinear Water Waves Generated by an Accelerated Circular Cylinder," Journal of Fluid Mechanics, Vol. 92, Part 4 (1979).

12. Haussling, H. J. and R. T. Van Eseltine, "A Combined Spectral Finite-Difference Method for Linear and Nonlinear Water Wave Problems," NSRDC Computation and Mathematics Dept. Report 27-74 (1974).

13. Haussling, H. J. and R. T. Van Eseltine, "Unsteady Air Cushion Vehicle Hydrodynamics Using Fourier Series," Journal of Ship Research, Vol. 20, No. 2 (1976a).

14. Haussling, H. J. and R. T. Van Eseltine, "Numerical Solution of Planing-Body Problems," DTNSRDC Report 76-0118 (1976b).

15. Haussling, H. J. and R. T. Van Eseltine, "Waves and Wave Resistance for Air-Cushion Vehicles with Time-Dependent Cushion Pressures," Journal of Ship Research, Vol. 22, No. 3 (1978).

16. Ohring, S., "A Fast Fourth Order Laplace Solver for Application to Numerical Three-Dimensional Water Wave Problems" (1975).*

17. Ohring, S. and J. G. Telste, "Numerical Solutions of Transient Three-Dimensional Ship-Wave Problems" (1977).**

18. Salvesen, N., "Ship Motions in Large Waves," Symposium on Applied Mathematics, dedicated to the late Prof. Dr. R. Timman, Delft University, The Netherlands (1978).

19. Salvesen, N. and C. H. von Kerczek, "Numerical Solutions of Two-Dimensional Nonlinear Body-Wave Problems" (1975).*

20. Salvesen, N. and C. H. von Kerczek, "Comparison of Numerical and Perturbation Solutions of Two-Dimensional Nonlinear Water-Wave Problems," Journal of Ship Research, Vol. 20, No. 3 (1976).

21. Salvesen, N. and C. H. von Kerczek, "Nonlinear Aspects of Subcritical Shallow-Water Flow Past Two-Dimensional Obstructions," Journal of Ship Research, Vol. 22, No. 4 (1978).

22. von Kerczek, C. H. and N. Salvesen, "Numerical Solutions of Two-Dimensional Nonlinear Wave Problems," Office of Naval Research Tenth Symposium on Naval Hydrodynamics, MIT (1974).

23. von Kerczek, C. H. and N. Salvesen, "Nonlinear Free-Surface Effects—The Dependence on Froude Number" (1977).**

**First International Conference on Numerical Ship Hydrodynamics, Washington, D.C. (1975).*

***Second International Conference on Numerical Ship Hydrodynamics, University of California, Berkeley, California (1977).*

profiles in science

Dr. John V. Wehausen is Professor of Engineering Science at the University of California at Berkeley and past Chairman of the Department of Naval Architecture. From 1946 to 1949 Professor Wehausen was a mathematician at the David Taylor Model Basin; and from 1949 to 1950 he was the Acting Head, Office of Naval Research, Mechanics Branch. In 1956, when Professor Wehausen went to the University of California at Berkeley, he was instrumental in establishing the Department of Naval Architecture. ONR, through research grants, gave substantial support to the new department. Many people in the Navy community today received their Ph.D.'s under the direction of Professor Wehausen, who encouraged Navy Laboratories and Bureaus to send their people to the Department of Naval Architecture for graduate work.

For many years the Office of Naval Research has funded Professor Wehausen's research in fluid mechanics especially in free surface flows and ship hydrodynamics. His pioneering accomplishments and many publications in these fields are world renown. He was among the first group of scientists to bring analytical methods to ship hydrodynamics. Professor Wehausen is a member of the Society of Naval Architects and Marine Engineers, American Mathematical Society, and the National Academy of Engineering.

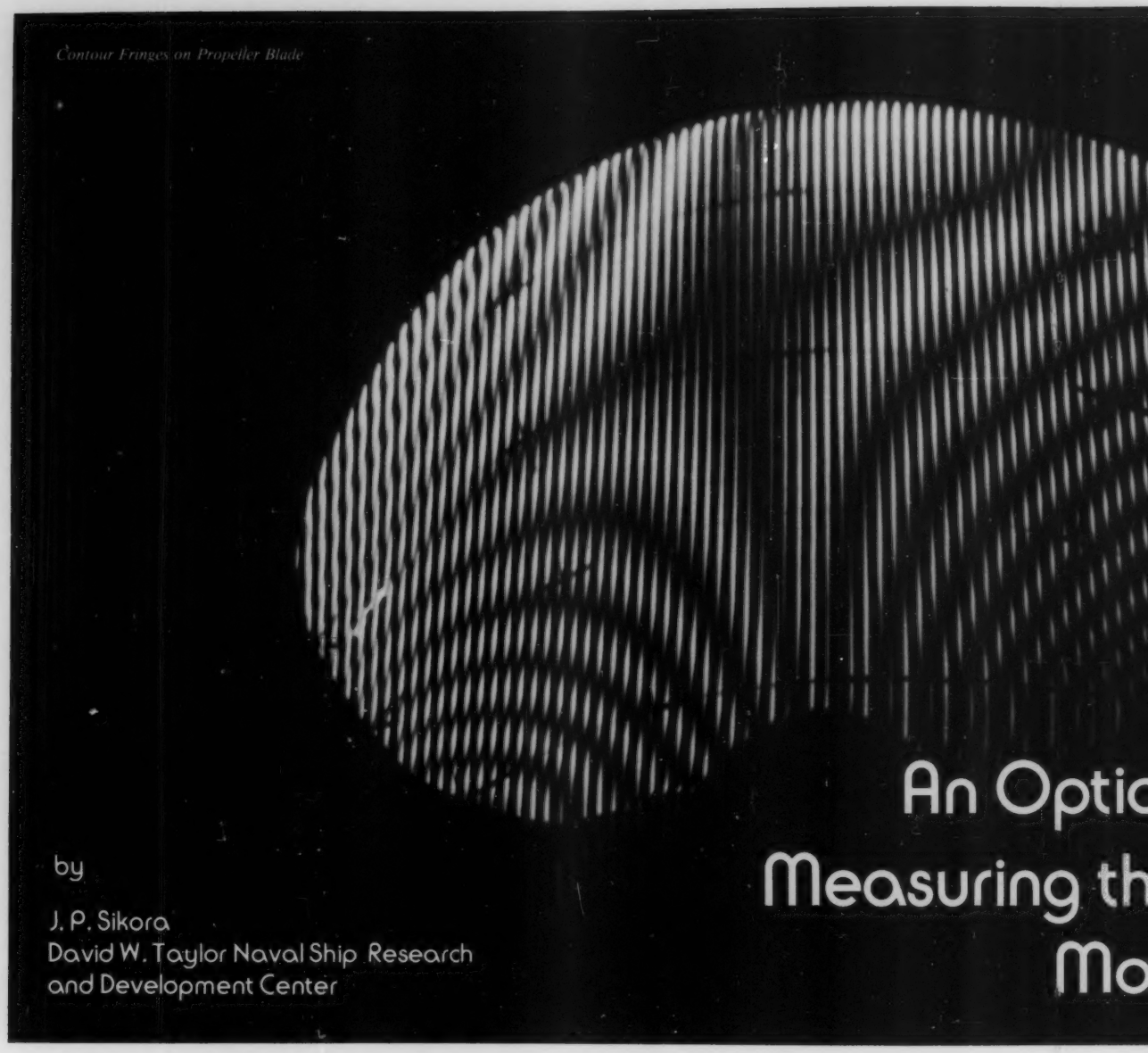

Contour Fringes on Propeller Blade

An Optic
Measuring th
Mo

by

J. P. Sikora
David W. Taylor Naval Ship Research
and Development Center

Although a propeller is conceptually a simple device to power a ship through the sea, it must perform its function as efficiently and quietly as possible. The U.S. Navy expends considerable effort to improve the hydrodynamic performance of its ships' propellers. Evaluations of improved propeller designs must also consider the propeller as a structural element to provide safe, reliable ship operations.

As a propeller responds to centrifugal and dynamic pressure loads, its blades deflect, thus altering the load distributions. The interaction between load and deflection in turbulent flow conditions encountered, for example, in backing and crash astern maneuvers cannot be reliably analyzed. Therefore, development of an experimental approach to measure the actual stresses and deflections of propellers operating underwater would be a significant aid to design

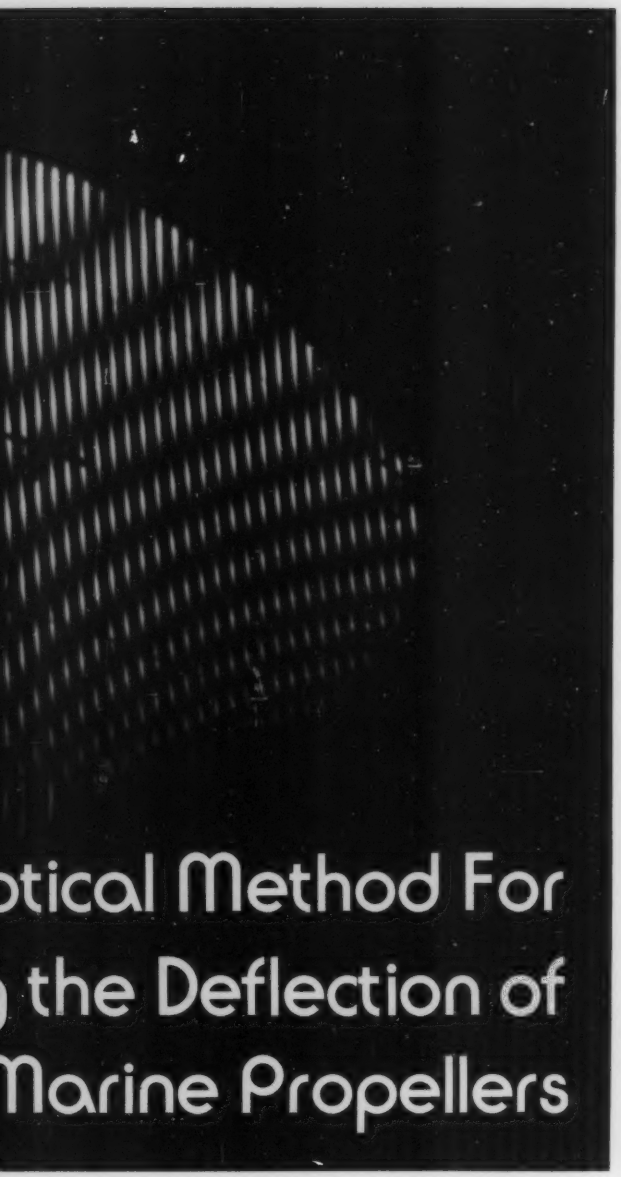

ptical Method For the Deflection of Marine Propellers

Mr. J. P. Sikora is a member of the Structures Department of the David W. Taylor Naval Ship Research and Development Center, Bethesda, Md. He has been engaged in the development of optical methods for structural mechanics and has published papers on holographic displacement analyses, the deflections of vibrating and rotating propellers, and fatigue crack growth studies.

efforts technique. This paper describes some results from an Independent Research Program (funded by the Office of Naval Research via the Director of Navy Laboratories) undertaken at the David W. Taylor Naval Ship Research and Development Center to develop methods to measure deflections of operating propellers.

Relatively few experimental methods have been successfully employed in the structural analysis of operating marine propellers. Strain gages may be used on operating propellers, but their installation on the blade surface can affect the flow patterns or alter blade response if the gages are recessed. Furthermore, the number of gages is usually limited because of difficulties in transferring the gage signal from the blade. A holographic approach[1] has achieved limited success; but, the sensitivity of holography is a disadvantage in the churning, vibrating, hostile environment of a water tunnel or open channel.

A promising method to measure the difference between a surface before and after deflection by a projected grid technique was first suggested by Hovanesian with others[2,3] and later expanded by Wasowski.[4] Deflections are simply obtained by comparing the initial shape of an object with its deformed shape. Although such projected grid techniques are much less sensitive than holography, they are also less disturbed by the environment and therefore were chosen for this study. Although these techniques had not previously been employed for rotating objects, they retain the advantage of being full-field and remote so as not to alter the flow around the propeller.

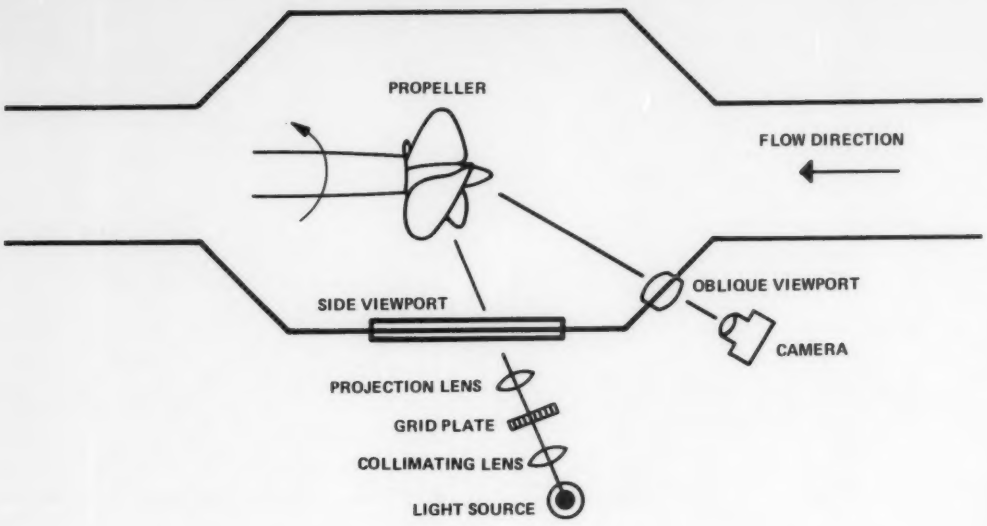

Figure 1—Optical Setup at Water Tunnel

Theory

The deflection of an object can be measured by a projected grid moire technique. Figures 1 and 2 depict a linear ruling or grid obliquely projected onto the surface of an object and photographed by a far-field camera. The point light source which projects the grid fills the space about the object with alternating planes of light and shadows (bright or dark bands). Every point illuminated on the object, therefore, is either in a bright band or a dark band. If a point P_1 in Figure 2 was initially photographed in a bright band and was then displaced to P_2 in a direction in line with the camera, P_2 will be either in a bright or dark band. Constructive interference occurs when P_2 is again photographed in a bright band, while destructive interference occurs when P_2 is in a dark band. Moire fringes of destructive interference can be observed in the double exposure photograph in regions which are deflected through 1/2, 3/2, 5/2, . . . bands of projected light. Constructive interference occurs at corresponding integer locations.

Referring to Figure 2, let the point light source be the origin of a polar coordinate system in a plane defined by the point light source, the camera lens, and the normal to the grid rulings.

Point P_1, originally at (r_1, θ_1), was deflected a distance Δ in the Y direction, one constructive interference phase shift to P_2 at (r_2, θ_2). Hence,

$$\Delta_{1,2} = r_1 \sin \theta_1 - r_2 \sin \theta_2 \tag{1}$$

Since $r_2 = r_1 \cos \theta_1 / \cos \theta_2$, and the angle β, subtended by adjacent planes, is the difference between θ_1 and θ_2, it can be shown that

$$\Delta_{1,2} = \frac{r_1 \sin \beta}{\cos (\theta_1 - \beta)} \tag{2}$$

Furthermore, the total deflection through n constructive interference fringes would be

$$\Delta_{1,n+1} = \frac{r_1 \sin (\pm n\beta)}{\cos (\theta_1 \mp n\beta)} \tag{3}$$

where + n (the number of interference fringes) is toward the camera and − n is away from the camera. From Equation (3), the deflection between successive interference fringes is not constant. However, in practice, r_1 is generally large and β is small, so the difference in deflection between successive fringes is often small.

For a far-field camera, the surface of the object can be assumed to lie in a plane. Thus, the distance p of Figure 2 can be related to the deflection Δ by

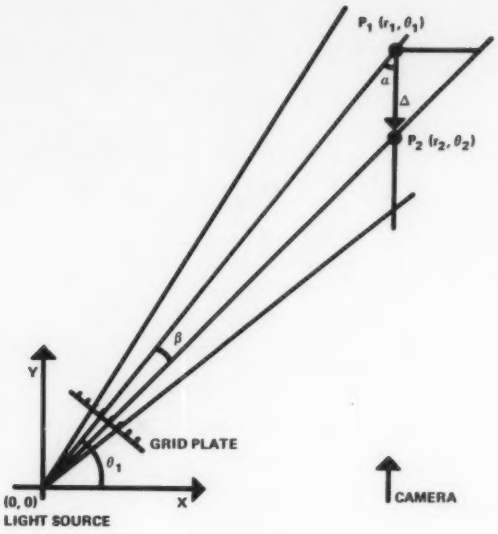

Figure 2—Schematic of Projected-grid Method

$$\Delta_{1,2} = \frac{P}{\tan(\alpha + \beta)} \tag{4}$$

In general, when β is small or the projected light is collimated ($\beta \equiv 0$), Equation (4) reduces to

$$\Delta_{1,n+1} = \frac{np}{\tan \alpha} \tag{5}$$

which is equivalent to the results from Hovanesian's, et al.,[2,3] analyses from light intensity considerations.

An alternative to making double-exposure photographs is to make a negative of the projected grid on the undeformed surface. Then, a second negative of the deformed surface is similarly made and the two negatives are superimposed as a sandwich. Moire fringes, as in the double-exposure method, will be apparent. This method is analogous to that of sandwich holography. To avoid in-plane rotational errors and lateral translations in this technique, it is helpful to include a second object that is not deformed in the scene so that markings on the second object can be accurately superimposed for proper registration.

Likewise, a contour map of the object can be obtained by comparing the surface of the object with a plane. A variation of the arrangement from Reference 2 is shown in Figure 3. Partial mirrors are placed in the path of the camera and projection system so that a reference plane can be seen superimposed on the object. The reference plane must be positioned such that the distance from mirror 1 to the object equals the distance from mirror 1 to the reference plane. Mirror 2 must also be equidistant from the object and reference plane. Under these conditions, the projected fringes on the object will interfere with those on the reference plane, thus producing a contour-difference map which can be evaluated by Equation (3). A left-to-right reversal of the reference plane is induced by the mirrors. This limits the method to comparing the object with plane or mirror-symmetric surfaces and requires that the projected grid lines be of constant pitch everywhere on the surface. Although the use of partial mirrors permits the contour fringes to be seen in real time or photographed with a single

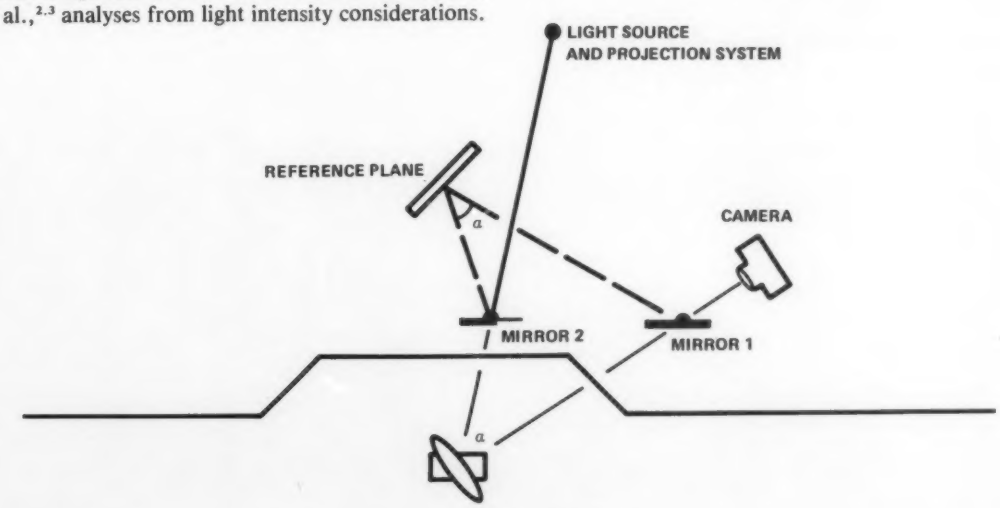

Figure 3—Contour-Difference Setup

exposure, the system is not very light efficient for dynamic applications. A double-exposure variation can be employed with standard mirrors that are removed between exposures. The contrast of the interference fringes can be further improved by using separate film plates for each exposure and then superimposing (or sandwiching) the negatives. With a judicious choice of projected grid lines, one can substitute the negative of the reference plane with a high quality master grid, further improving the contrast of the interference fringes.

Experiment

As a first step toward measuring the deflections of a propeller rotating in a water tunnel, deflections of a propeller rotating in air were measured. A plastic, rectangular blade, 254 mm diameter × 25 mm × 3 mm with eccentric masses 12 mm from the blade tips, was rotated at speeds up to 900 rpm by a d.c. motor. Figure 4 shows the experimental setup. A laser beam was reflected from a mirror on the motor shaft onto a photodetector 4.3 m away. The photodetector triggered a flash strobe which projected a grid of 1.46 lines/mm onto the rotating blade when it was in the desired angular position. The first exposure was made while the blade rotated slowly. The blade speed was then increased and the photodetector advanced, so that the second exposure would occur with the blade in the same angular position. Photographs of the moire fringes on the blade at 480 and 756 rpm are shown in Figure 5. The displacements along the centerline of the blade were measured and are plotted in Figure 6 along with those from a finite element analysis. A power function was fit by least squares criteria to the displacements at each speed. Strains and stresses were then calculated from the second derivative of the functions and are plotted in Figure 7 along with those from the finite element analysis.

Thus, having established the validity of the technique for rotating objects, a three-bladed, left-handed, 24.4 cm diameter, aluminum, marine propeller (Figure 8) was mounted in a 0.9 m variable pressure water tunnel. Figure 9 shows the optical setup at the water tunnel. A flash strobe projected a grid of 0.53 lines/mm onto the propeller through one of the water tunnel's side viewing ports and a camera was mounted to photograph the propeller through one of the small oblique viewing ports. (The oblique viewing ports contained correction lenses for air-water aberrations.) Because of the fixed position of the oblique ports and the location of the tunnel nozzle, the entire surface of one of the blades could not

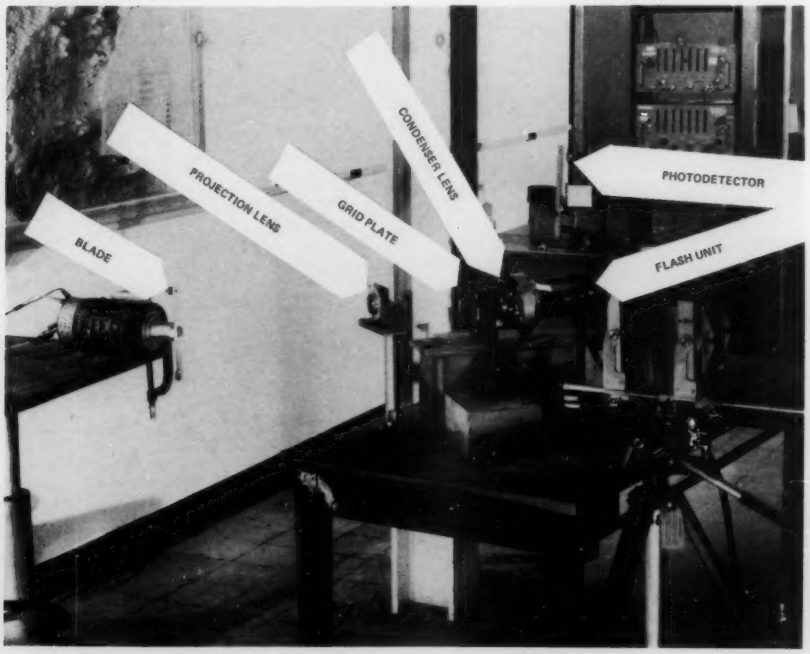

Figure 4—Experimental Setup for Propeller Rotating in Air

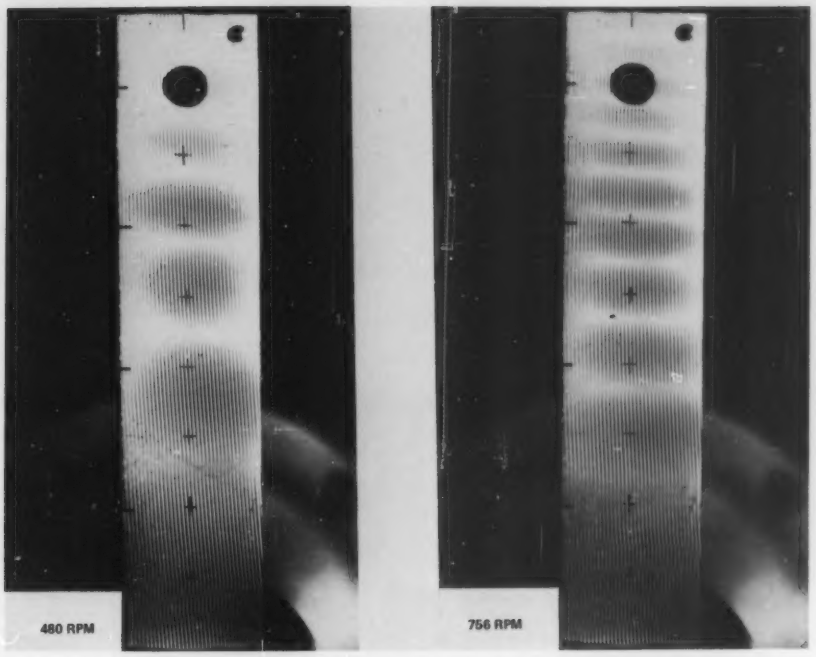

Figure 5—Deflection Fringes on Propeller Rotating in Air

be photographed while the blade was normal to the camera. An available magnetic pickup on the propeller shaft was used to trigger the flash strobe when the propeller was in the desired angular positions.

Figure 10 shows the moire deflection fringes on the propeller rotating at 1000 rpm underwater. The blade was loaded by varying the flow velocity (up to 15 m/s) in the tunnel between the two exposures. This corresponds to the crash ahead and crash astern load conditions, with the thrust loads on the propeller reaching 4900 N.

Figure 11 is a plot of the steady state blade deflections along the midchord radius line. Difficulties with the triggering device precluded varying the rotational speed of the propeller while maintaining the flash at the same angular position as in the case of air. Double-exposure photographs were also made of the propeller rotating at 500 and 2000 rpm.

The shape of the propeller was measured by the previously described contour difference method depicted in Figure 3.

The lead photograph of this article on page 20 is of the contour fringes on the propeller at rest. Since the shape of the propeller relative to a plane involves greater distances than the deflictions, a coarser projected grid was employed resulting in interference fringes of sharp contrast.

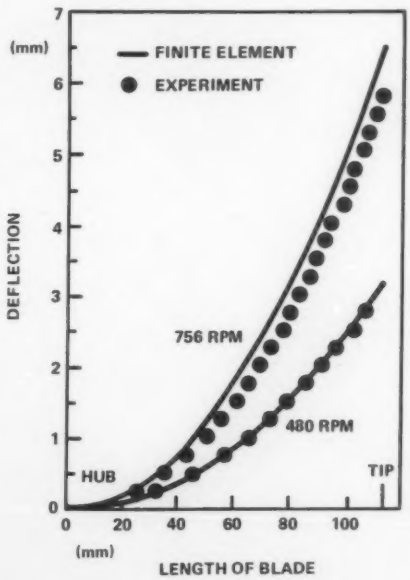

Figure 6—Blade Deflections of Propeller in Air

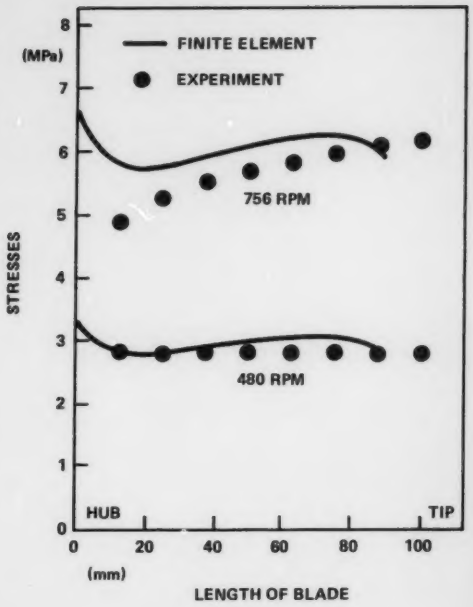

Figure 7—Blade Stress of Propeller in Air

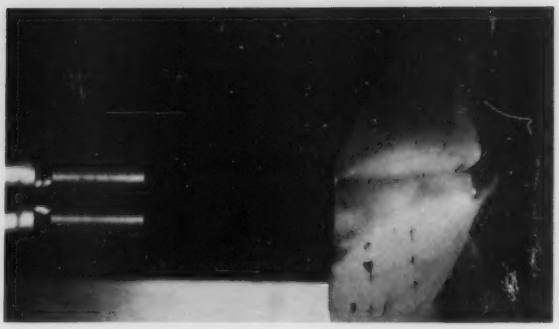

Figure 8—Propeller Inside Water Tunnel

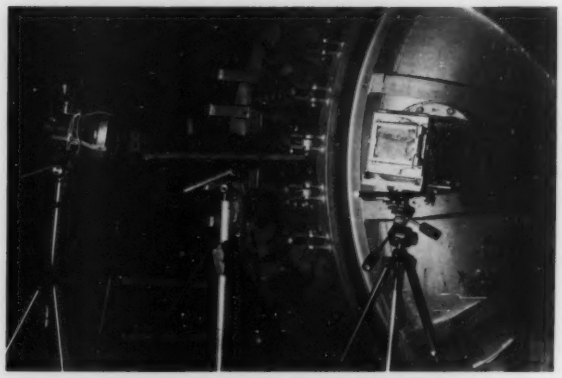

Figure 9—Experimental Setup at Water Tunnel

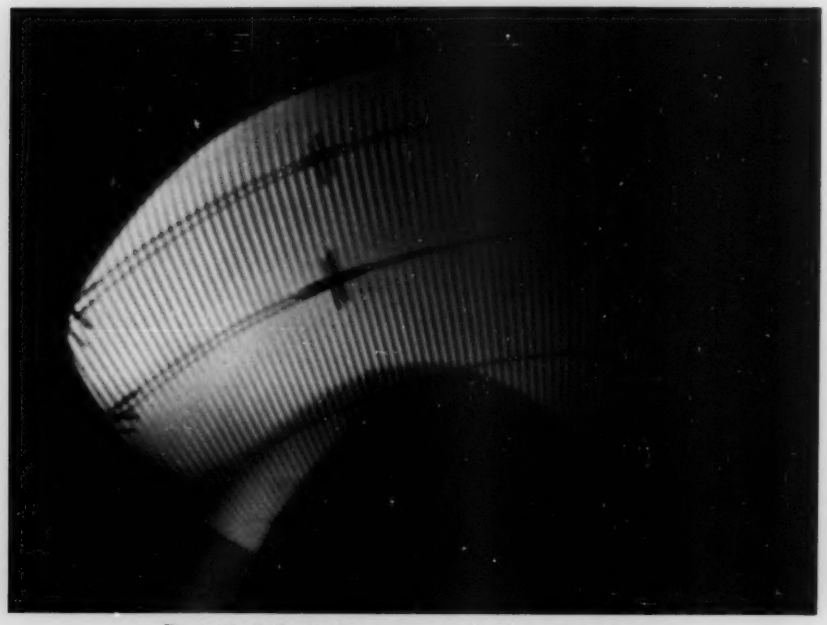

Figure 10—Deflection Fringes on Propeller Rotating Underwater

Because of the curvature and varying pitch of the propeller, not all parts of the blade deflected in line with the camera. This, together with the fixed position of the camera because of the viewing ports, results in the dual images seen along the trailing edge of the blade in Figure 10. Although the viewing port diagonally across the tunnel had a somewhat better view, cavitation bubbles obscured that face of the blade. (Cavitation bubbles can also be seen trailing from the silhouetted blade in the foreground of Figure 10.) The contour difference method would be most useful on a propeller of uniform pitch provided that the camera could view in a normal direction to the pitch angle.

This program was initiated under Independent Research sponsorship in FY 78 and has since been sponsored by the Independent Exploratory Development program at the Center.

Conclusions

An optical method has been developed to measure the deflections of rotating propellers in a water tunnel environment.

Advantages of the method include being full-field and noncontacting, requiring no extensive or exotic apparatus, requiring no special surface preparation or materials, and being able to be used in hostile environments (e.g., turbulent water). If good quality photographs, either motion picture or flash, can be made of the structure during its loading, then a deflection analysis can be performed. As in any experimental endeavor, limitations due to timing synchronization, light intensity, photographic resolution, and physical accessibility must always be considered.

The fine quality of the photographs showing the moire interference fringes demonstrates the feasibility of using such underwater measurement techniques. Vibrations of the shaft and tunnel, as well as particles and entrapped air in the fluid, were not found to be detrimental to the method. Good agreement with analytical results confirms the accuracy of the method. The simplicity of the method in obtaining full-field data is an important consideration to future full-scale propeller deflection measurements at sea. Another potential benefit to the Navy is the ability to measure propeller response under steady state and transient load conditions which approach the ultimate strength of the propeller. ■

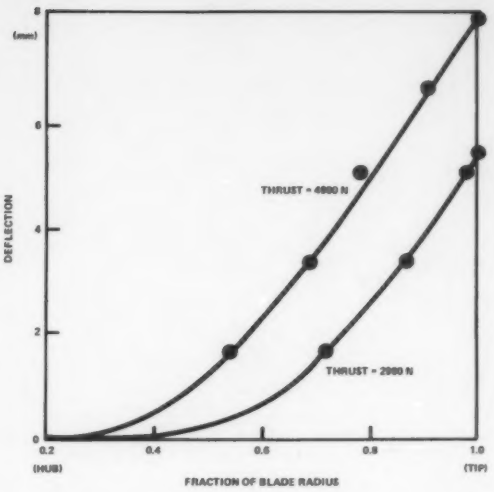

Figure 11—Blade Deflections of Propeller Rotating Underwater

References

1. Sikora, J. P., "Structural Analysis of Propellers Rotating Underwater Using Holography," Proceedings of the SNAME Symposium-Propellers '75, Philadelphia, Pa. (1976).

2. Hovanesian Der, J., and Y. Y. Hung, "Moire Contour-Sum Contour-Difference and Vibration Analysis of Arbitrary Objects," Applied Optics, Vol. 10, No. 12 (1971.)

3. Hovanesian Der, J., R. E. Haskell and R. L. Powell, "Use of a Projected-Ruling Moire Method for Vibration and Deflection Measurements of Three-Dimensional Structures," Proceedings of the Symposium-Engineering Applications of Holography, Los Angeles, Ca. (1972).

4. Wasowski, J. J., "Moire Surface Contouring by Addition Method," Proceedings of the Sixth International Conference on Experimental Stress Analysis, Munich, W. Germany (1978).

Lasers for Hydrographic Applications

by

M. B. White
Office of Naval Research
Eastern/Central Regional Office

Introduction and Background

Coastal hydrography, the measurement and charting of ocean depth near the coast line, is of great importance in maintaining safe, navigable waterways for military, commercial and recreational utilization. The traditional method for obtaining hydrographic data is to make "lead-line" and acoustic soundings from low-speed launch craft. This method is so slow and expensive that it does not appear capable of supplying hydrographic data for all coastal areas of high interest on any reasonable time scale. It is estimated by the Defense Mapping Agency that there currently exists a two-hundred ship-year backlog for charting foreign waters, and that 75 percent of the charts that do exist are inadequate!

For over ten years programs have been pursued by a number of western nations (including the U.S., Australia and Canada) to probe the feasibility of utilizing aircraft-borne optical radar (i.e., lidar) to expedite the hydrographic data collection process. In the U.S., the first experimental field demonstration of this approach was carried out, under NAVOCEANO sponsorship, in 1969. Since then, a number of

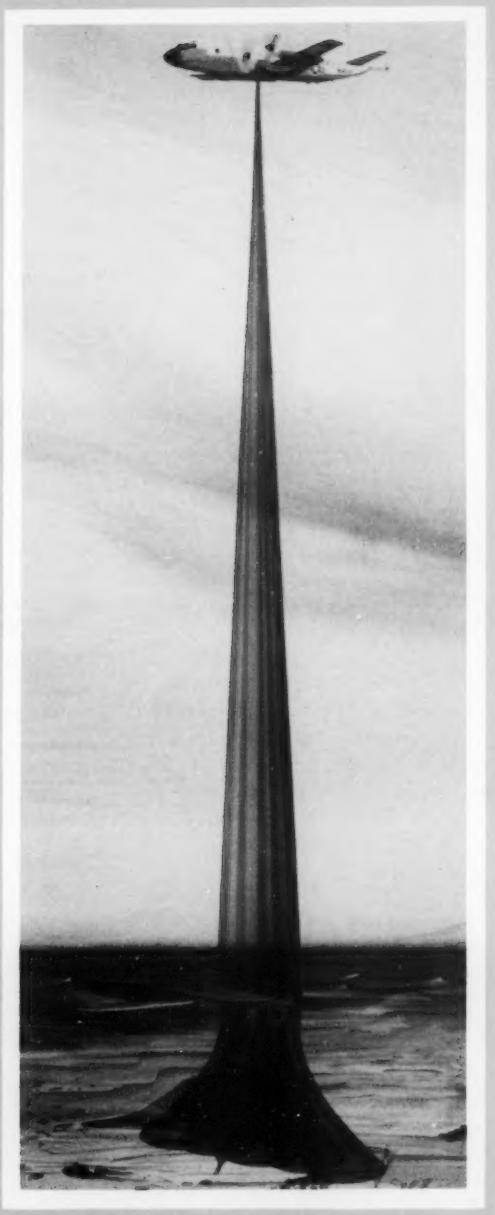

Figure 1. Aircraft-Borne Lidar Hydrographic System Operation–5 ns pulses from a 400 pps, 2 mJ/pulse green laser are projected from a small aircraft onto the ocean in a scan pattern. Pulse reflections from the surface and bottom are detected, using an aircraft-mounted PMT/Logamp, and water slant-depth is determined from the difference in platform-to-surface and platform-to-bottom optical pulse transit times. Aircraft horizontal coordinates are determined using standard electronic positioning equipment with RF-emitting shore stations.

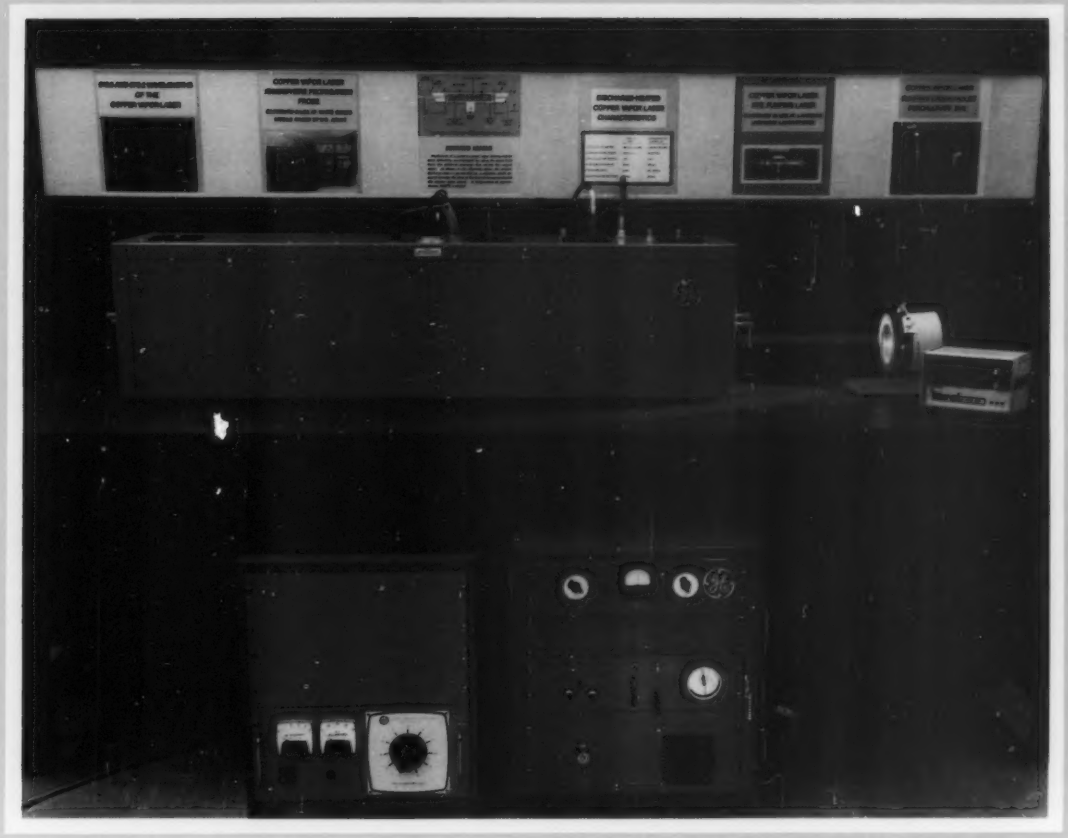

Figure 2. General Electric Company Model 6-15 Copper Vapor Laser–This commercial laser produces 15W of average optical output power at a 6kHz PRF with a maximum input electrical power consumption of 3KW. Output pulse width is 30 ns. In the photograph, the green 2.3 cm diameter output beam from the laser is shown impinging upon a power-meter. All the auxiliary electrical drive equipment necessary for operating the laser is stowed under the laboratory bench.

increasingly sophisticated lidar hydrographic systems have been developed and field-tested. This has allowed both technical and economic issues to be analyzed in great detail.

The most recent U.S. initiative in the hydrographic lidar area is the DMA/NORDA Hydrographic Airborne Laser Sounder (HALS) System. This system will be delivered to NAVOCEANO for field-testing in early 1982, and it should be ready for routine operational soundings sometime in 1983.

The basic operational principal of all aircraft-borne lidar hydrographic sounding systems is shown schematically in Figure 1. In the arrangement shown, very short (<5ns) green output pulses from an aircraft-mounted laser are projected onto the ocean surface. Water slant depth (along the laser beam propagation direction) is calculated by noting the round-trip pulse transit times for ocean surface and ocean bottom reflections. Rapid data acquisition is made possible by operating the laser source at high-pulse-repetition rate (400 Hz) and scanning the projected light beam.

Recently, the National Ocean Survey (NOS) performed a detailed operational/economic analysis of the impact that use of an airborne lidar hydrographic system could have on its ability to carry out its CONUS hydrographic charting responsibilities. It was concluded that by using a lidar system similar to HALS on a small fixed-wing aircraft, the cost-per-unit-area of NOS hydrographic chart production could be cut by a factor of six, and the time-per-unit-area for obtaining the required depth data could be decreased by more than a factor of one hundred. This

Figure 3. Naval Ocean Systems Center Mercury Bromide Dissociation Laser–The laser is pictured with the top of its white, firebrick oven-assembly removed so that the quartz laser tube can be seen. The bright white spots along the top of the discharge tube are spark discharge sources used to produce UV radiation for preionization. The 30-inch-long screen anode of the main transverse discharge system appears as a white streak below the preionizers. The blue-green laser output beam leaves the discharge tube through an upward-facing quartz Brewster window, passes out of the laser cavity through a gimbaled, semi-transparent mirror, and impinges upon a remote power-meter. This laser produces 3W of average optical power at a 100 Hz PRF with an overall efficiency of 0.7 percent.

means that one such lidar system could collect more data-per-year than the entire NOS fleet currently collects! The results of this NOS analysis, as well as similar conclusions reached by other workers in the hydrography area, make it abundantly clear that use of aircraft-mounted lidar constitutes the best, and probably the only, way to supply present and envisioned needs for ocean bottom topographic information.

In laser hydrographic applications the water depth is determined by measuring the difference in transit times for optical pulses reflected from the ocean surface and bottom. Therefore, it is necessary that the spatial lengths of the laser pulses used be of the same order, or smaller than, twice the required hydrographic depth accuracy (of 30 cm). This limits the temporal pulse length to 5 ns or less. Furthermore, since a practical airborne lidar hydrographic system will normally operate from a small helicopter or fixed-wing aircraft, the laser must be small, light, and have an electrical power requirement of at most a few kilowatts. The required pulse-repetition-rates range from a few hundred Hertz, for hydrographic sounding in CONUS and friendly foreign waters, to ten kilohertz or more for soundings along hostile coastlines during military operations. Pulse energy requirements are modest ($\approx$1-5 mJ) because of the shallow waters and modest aircraft altitudes involved. The preferred output wavelength is green to yellow-green because of the transmission characteristics of the murky, organism-laden coastal waters in which hydrographic systems generally operate. The HALS System specifications of Table I are representative of near-term hydrographic laser requirements.

In contrast to hydrographic laser applications, most military ocean-optics systems involve optical transmission over long paths through relatively clear open ocean waters. Consequently the laser needs associated with these systems are significantly different from the hydrographic laser requirements indicated in the discussion above and in Table I. Nevertheless, many of the new, promising laser concepts that have been under vigorous exploratory development in the U.S. over the last few years for under-

Figure 4. Naval Research Laboratory Raman-Downshifted Xenon Chloride Laser–In this arrangement an invisible beam of 308 nm UV radiation leaves the xenon chloride laser cavity through its gimbaled output mirror (small doughnut-shaped object in upper left of photograph). This UV beam enters a heated lead-vapor cell that is mounted in a firebrick-oven assembly (large white rectangular box). Stimulated Raman Effect in the lead vapor frequency-downshifts the UV radiation, producing a blue light-beam. This beam leaves the lead-vapor cell, through a water-cooled quartz window, and strikes a remote translucent glass plate (lower right of photo). A UV-to-blue down-conversion efficiency of over 50 percent has been achieved using this arrangement.

water communication, ranging, and detection could, in principle, be directly adapted for hydrographic use on a two-to-five year time scale. Also, there is a small but active ongoing basic/applied research effort in the U.S. that is specifically directed toward hydrographic laser development.

Some of the most promising future hydrographic laser possibilities are discussed below. These candidates can, for the most part, be classified as being of metal-vapor, molecular-gas, or solid-state types. They all appear capable of satisfying hydrographic radiation output requirements in small, light-weight, highly reliable configurations of a type suitable for aircraft mounting.

Copper Vapor Laser

The copper vapor laser shows great promise of providing a significant near-term advancement in the hydrographic laser state-of-the-art. In its usual mode of operation, this device produces 20-40 ns output pulses at pulse-repetition-frequencies between 1 and 15 kHz. The output normally contains spectral components at 511 nm and 578 nm, with about two-thirds the energy in the 511 nm line.

In the early 1970's, two alternative types of electrical-discharge-excited Cu vapor lasers were pursued with about equal vigor. One type uses pure metallic copper as the active lasing material, while the other uses a copper halide such as CuCl or CuBr. The pure copper device has the advantage of higher output energy-per-unit-volume but has to operate at 1500°C, where common discharge tube fabrication materials and sealing techniques cannot be used. On the other hand, the copper halide laser can operate at tempera-

Output Wavelength	531 nm
Pulse Energy	2 mJ
Pulse Length	5 ns
Pulse Repetition Rate	400 Hz
Max. Electrical Input Power	5 kW
Max. Volume	2 m^3
Max. Weight	400 kg
Mean Time Between Failure	100 hr

Table I. Hydrographic Airborne Laser Sounder (HALS) Requirements

tures where simple fused silica discharge-tube technology is applicable (400°-600°C) but is limited in its volumetric energy density and pulse-repetition-rate capabilities. By operating in a mode where waste heat from the electrical discharge is used to vaporize the Cu or Cu halide, both types of copper lasers can routinely achieve "wall-plug" electrical-to-optical energy conversion efficiencies of over 1 percent.

The operational lifetimes of copper vapor lasers are normally limited by seal integrity and/or diffusion of the Cu or Cu halide out of the hot active-gain region of the discharge tube. This is a particularly severe problem with the metallic copper laser because of its very high operation temperature. Nevertheless, metallic Cu systems have been operated in the U.S., for over 700 hours, by using a slow gas-flow to compensate for seal leakage. Over 3000 hours of continuous sealed-off operation has been achieved in the Soviet Union by employing a high buffer gas pressure to impede the diffusion of Cu atoms out of the discharge region.

Because Cu halide devices operate at temperatures where an "all hot" quartz configuration is premiseable, it is fairly straightforward to realize a simple, He-Ne laser type of design which is much less plagued by seal and gas diffusion problems. Such devices have been operated, sealed-off, for several hundred hours with no measurable decrease in output power.

Primarily because of the energy/pulse requirements of most systems applications, recent U.S. copper laser development efforts have for the most part concentrated on the use of pure metallic copper in a longitudinally excited configuration. Over one hundred such lasers, with the output specifications shown in the first column of Table II, have been sold by the General Electric Company. A photograph of a 15W average power device that is offered commercially by G.E. is shown in Figure 2. Longitudinally excited copper vapor lasers that deliver over 55 watts of average power have been demonstrated in the laboratory.

Longitudinal discharge, low-pressure copper vapor lasers are generally limited to volumetric output energy densities of $\sim$10 μJ/cc/pulse. However, by converting to a higher pressure gain medium and transverse-discharge pumping, both higher energy density and higher electrical efficiency appear to be possible. Soviet scientists report that, using this approach, they have demonstrated energy densities of 640 μJ/cc/pulse and efficiencies of 2.5 percent.

As is implied by the discussion above, already demonstrated copper vapor laser technology would be nearly ideal for high-data-rate hydrographic sounding applications, if the 20-40 ns pulse-widths that normally characterize such lasers were about an order-of-magnitude shorter. In view of this fact, a U.S. Navy-supported research program was initiated about two years ago at the G.E. Applied Sciences Laboratory to try to devise a simple technique for obtaining short pulse copper vapor laser output. The goal of the program was to demonstrate a metallic copper vapor laser with the output characteristics shown in the second column of Table II. The characteristics shown in the third column were subsequently demonstrated.

The initial approach followed by G.E. involved

Table II. General Electric Copper Lasers

	Commercial Product	Hydrographic Laser Goals	Hydrographic Laser Demonstrated
Average Power	5 W	6 W	5.6 W
Pulse Energy	800 μJ	400 μJ	700 μJ
Pulse Repetition Rate	6 kHz	15 kHz	8 kHz
Pulse Length	20 ns	3 ns	5 ns
Electric Input Power	1 kW	1 kW	3 kW

the use of a short copper "laser" with only one cavity mirror. It was found that although this double-pass amplified fluorescence configuration was capable of producing the requisite pulse-width and energy-per-pulse, the angular divergence of the resulting light-beam was too large for the intended hydrographic sounding application. The output characteristics listed in column 3, Table II, were finally obtained with low (∿1 mrad) beam divergence by using a two-mirror true laser configuration and carefully adjusting the copper density, buffer gas pressure, and drive voltage. It is interesting to note that, for the laser configuration used by G.E., the observed five ns pulse length corresponds approximately to the time necessary for light to travel one round-trip through the cavity!

A contract to deliver a ruggedized version of the G.E. hydrographic copper laser for airborne field experiments is presently in progress.

Near-Atmospheric-Pressure Molecular Gas Lasers

Over the last several years an entirely new class of UV and visible near-atmospheric-pressure molecular gas laser (MGL) has been under rapid development in the U.S. and elsewhere. These lasers all require short, very high voltage electrical pulses for transverse excitation and all require UV preionization of the gas mixtures involved for stable operation. The molecular-chemistry/electron-kinetics involved in the operation of these lasers is generally very complex, and entails a multiplicity of electron excitation/ionization and molecular energy-exchange processes. In all cases the lower laser state is unstable because of molecular recombination and/or dissociation. Hence, an automatic population inversion results. Because of the very short lifetimes of the excited molecular levels involved, all MGLs operate only in the pulsed mode, with pulse lengths ranging from 10's to 100's of nano-seconds. UV-producing MGLs are available commercially from a number of manufacturers. These typically provide 40-50 ns, 50-100 mJ pulses at 10 Hz pulse-repetition-frequencies.

Without doubt, the leading MGL candidates for hydrographic applications are the electrically excited mercury bromide dissociation laser, which operates directly in the green portion of the spectrum, and the xenon chloride excimer laser, which produces UV output that can be efficiently frequency-down-converted to the green. Because of their great promise for use in hydrographic systems and their relatively high levels of development, these MGLs are singled out for more detailed description in the paragraphs below.

Dr. White is an electro-optical physicist at the Office of Naval Research Eastern/Central Regional Office, Boston. He serves as ONR focal point for blue-green lasers and ocean-optic oriented activities and is the ONR manager for the Navy/Defense Advanced Research Projects Agency Program.

Mercury Bromide Dissociation Laser

The upper level of the mercury bromide dissociation laser is an excited state of the HgBr molecule, which is formed as a result of electrical discharge dissociation of (stable) $HgBr_2$. After stimulated emission, the resulting HgBr ground-state molecule quickly recombines with a free bromine atom to reform the original $HgBr_2$ molecule. During this cyclic molecular process, the lower laser level is rapidly depleted so that the population inversion necessary for laser operation can be achieved. Also, since all dissociated $HgBr_2$ is ultimately reconstituted, the possibility for long-life sealed-off laser operation exists.

The mercury bromide laser normally operates over a broad wavelength band stretching from 490 nm to 510 nm. However, by injecting a weak narrow-band optical signal into the laser cavity (i.e., by "injection locking") it is possible to operate at any wavelength within this band with an output linewidth of less than 0.05 nm. In order to achieve the required $HgBr_2$ vapor pressure for laser operation, the system must be held at a temperature exceeding 170°C. It has been demonstrated that this temperature can be maintained quite easily by using waste heat from the discharge, in the same manner as was described above in connection with the copper vapor laser. U.S. Navy

researchers at the Naval Ocean Systems Center have operated a sealed-off "self-heated" mercury bromide laser for 10^6 pulses at 100 pps. Three watts of average power were achieved at 0.7 percent efficiency. A photograph of the laser that was used is given in Figure 3.

Low pulse-repetition-rate mercury bromide lasers have been operated with over one percent wall-plug electrical-to-optical energy conversion efficiency and output energy densities of 1 mJ/cc/pulse. There does not seem to be any inherent reason why "scaling down" to the 1 mJ/pulse required for hydrography should present any particular problem. As is the case with all MGLs, the presence of highly reactive gases in the mercury bromide laser discharge makes it very difficult to avoid chemical reactions with the electrodes and other metallic parts of the system. This, in turn, could make it extremely difficult to achieve the very long ($\approx 10^9$–10^{10} shot) operational lifetimes required for some military applications. However, in the case of hydrographic sounding, where the laser can be serviced every few hours, these slow chemical degradation effects should not constitute a serious problem.

It should be noted that although most mercury halide laser development work has concentrated upon the mercury bromide laser (because its output wavelength is appropriate for penetration of clear ocean water) there is every reason to believe that the mercury chloride dissociation laser could be further developed to provide performance that equals or surpasses that achieved with mercury bromide. It is therefore very likely that most of the rapidly accruing mercury bromide laser technology could be directly transferred to produce a mercury chloride laser with output in the 555 nm-565 nm wavelength range. Such a laser might prove very useful for hydrographic measurements in murky coastal waters.

Raman Downshifted Xenon Chloride Laser

The xenon chloride MGL, which produces an ultra-violet output wavelength of 304 nm, is probably the most highly developed of all MGLs. This device has been operated at a 1 kHz pulse repetition rate to produce 210 watts of average power at over one percent efficiency. A continuous lifetime of 10^8 shots has been obtained from a sealed-off laser with rapid gas recirculation, and a wavelength tuneability of tens-of-nanometers has been demonstrated with an output linewidth of .01 nm. Output energy densities of several mJ/cc/pulse are readily achieved. A program is presently underway to develop a XeCl laser which produces several hundred watts of average power and is capable of a very long operational lifetime.

The reason for the great interest in (and therefore the rapid development of) the xenon chloride laser is that its 304 nm output wavelength fortuitously coincides with an atomic resonance transition of Pb. This coincidence allows the Stimulated Raman Effect to be used to very efficiently downshift the UV laser output wavelength to the blue-green (459 nm) region, where it can be advantageously used for ocean-optics applications (such as hydrography).

Using a simple experimental arrangement in which 50 mJ output pulses from a XeCl laser were focused into a heated cell containing lead vapor, workers at the U.S. Naval Research Laboratory have achieved 50 percent energy-conversion efficiency from the UV to the blue-green. A photograph of the apparatus used is given in Figure 4. There is little doubt that a scaled-down version of this arrangement could provide a useful low PRR blue-green source, with lifetime capabilities consistent with hydrography mission length requirements.

Because of the highly corrosive nature of hot lead vapor, the development of a lead vapor Raman Effect wavelength converter with a very long operational life could prove to be a difficult technical problem. For this reason, there is an effort underway to develop UV-to-blue-green Raman Effect downshifting techniques that involve less corrosive room-temperature gases. These techniques all involve multiple Raman Effect downshifts in one or two molecular gases contained either in one cell or in sequential cells. Multiple shifts are necessary because, for molecular gases, the wavelength change for a single shift is too small to convert from the UV to the green. For example, three Raman Effect downshifts of XeCl laser output in hydrogen gas produce green radiation at 500 nm, while two downshifts in hydrogen and one in deuterium provide blue-green radiation at 472 nm. Since a multiplicity of non-resonant Raman Effect shifts is involved, the overall efficiency of the molecular gas downshifting process is not expected to be as high as what could be obtained using a single resonant Raman Effect downshift in atomic lead (30 percent vs 50 percent observed). However, the molecular process has the advantage of providing a potentially long-lived system, and of allowing some selectivity of the final wavelength (through choice of the Raman Effect downshifting gases). This selectivity could be of considerable significance for hydrography.

Ultra-violet Molecular Gas Laser Pumped Lasers

For many years UV gas-laser-pumped dye lasers have been commercially available from many manufacturers and have been widely used as tuneable visible sources for spectroscopic measurements. Use of coumarin and rhodamine dyes allows these systems to be tuned through the entire yellow and green regions of the spectrum, with 30-50 percent UV-to-visible energy conversion efficiency. The output pulse length is determined by that of the pump laser. It can range from five-to-fifteen nanoseconds, for a nitrogen laser pump, to continuous wave for rare-gas ion laser pumps.

The primary reason that UV gas-laser-pumped dye lasers have not been used for field applications, such as hydrographic sounding, is that the very low electrical efficiencies of available UV pump lasers precluded such utilization. For example, the commonly employed UV nitrogen laser is characterized by an electrical-to-optical energy conversion efficiency of only a few one-hundredths of one percent. With the emergence of UV molecular gas lasers that have potential efficiencies of several percent, renewed attention is being given to the use of UV laser-pumped dye lasers for field applications. There are apparently a number of applications where the wavelength agility afforded by such devices trades off favorably against the added complexity of a compound laser source.

In addition to being potentially useful for pumping green dye lasers, UV MGLs are also strong contenders for pumping green and blue-green gas and solid-state lasers. For example, the first mercury bromide dissociation laser was photolytically pumped using UV output from an ArF MGL. A program has just been initiated to optically pump a Xe_2Cl laser (λ = 478 nm) using 308 nm UV output from a XeCl MGL. Furthermore, it has been demonstrated that the Tm:YLF solid-state laser (λ = 452 nm) can be optically pumped, very efficiently, using output from a 351 nm XeF MGL. Sixty percent UV-to-visible energy conversion efficiency appears to be possible using this approach.

Short Pulse Operation Of Molecular Gas Lasers

Molecular gas lasers generally produce pulses with lengths ranging from thirty to several hundred nanoseconds. Therefore, in order to provide the ± 30 cm ocean depth accuracies required for hydrographic applications, special techniques must be used to reduce the normal pulse lengths to the three-to-five nanosecond range (see discussion in Introduction and Background section).

There is every reason to believe that the "cavity dump" approach that has been used to obtain short pulse output from solid-state and dye lasers could be applied equally well to gas lasers. Attempts to demonstrate this experimentally with the mercury bromide and the copper vapor laser are in the planning stage at NOSC and NADC, respectively. With the "cavity dump" approach, the laser radiation is stored in a high "Q" resonant cavity until peak intracavity intensity is reached, and is then dumped out, using a fast electrooptical shutter. Theoretically, an output pulse length equal to twice the laser cavity length should be achievable. In fact, the pulse length is usually determined by the frequency response of the electrooptical shutter drive circuit.

Another technique that can be used to extract short-pulse output from an MGL is to utilize a master-oscillator-power-amplifier (MOPA) configuration, with the oscillator electro-optically short-pulse-gated and the amplifier traveling-wave excited. Since most of the final output energy is extracted from the amplifier, the energy that is thrown away in gating the oscillator output pulse has a minimum effect on overall system efficiency. By using traveling-wave electrical excitation of the amplifier to create an amplifier population inversion that is temporally synchronized with passage of the pulse from the oscillator, optimum short-pulse amplifier extraction efficiency is obtained with minimal loss to superfluorescence. This MOPA approach has been used successfully with the $He\text{-}N_2$ charge-transfer gas laser. Similar MGL MOPA configurations are under study at a number of United States laboratories for solving high-energy MGL frequency selection and beam-control problems.

A very promising short-pulse MGL configuration, that has recently been demonstrated at the United Technologies Research Center in East Hartford, Connecticut, appears to be particularly well suited for hydrographic sounding applications. In this configuration, the active laser gas is contained in a small capillary tube ($\approx$30 cm long, .5-1 mm bore) and is longitudinally excited using a pulsed capacitive discharge. Because the discharge tube is so small, system inductance is naturally very low and short-pulse output is easily achieved. The system is inherently simple and compact, and would appear to lend itself very well to operation from a small airborne platform. Although the small capillary discharge volume limits output to $\approx$1 mJ/pulse, this output energy is

large enough for most hydrographic sounding applications.

So far, the UTRC capillary discharge configuration has been used to obtain laser action from four different MGL species, including xenon chloride and mercury bromide. Best results have been obtained using KrF (λ = 248 nm), where 50 uJ, 3 ns pulses were obtained from a 0.04 cc gas volume with 1.5 percent efficiency.

Green Solid-State Lasers

In addition to the highly developed frequency-doubled Nd:YAG laser, which represents the state-of-the-art in hydrographic laser technology, there are a number of advanced solid-state laser options that show great promise. In particular, several solid-state laser candidates that directly provide output in the green are in the early phases of development. Use of such lasers would eliminate the need for a frequency doubler, thereby greatly decreasing the complexity and increasing the reliability of optical hydrographic systems.

Measurements of the 550 nm stimulated emission cross-section of liquid-nitrogen-cooled Er:YLF have just been completed at MIT. The results of these measurements strongly indicate that efficient green laser operation should be possible using that material. An attempt to verify this conjecture experimentally is underway. Since a well-engineered liquid-nitrogen-cooled infrared solid-state laser is commercially available, packaging of a very similar 77°K Er:YLF laser for airborne hydrographic applications is not expected to constitute a difficult problem.

Strong theoretical evidence exists that the use of Ce:ThO_2, in a laser configuration similar to that commonly used for Nd:YAG, should result in an efficient room-temperature solid-state laser that is tuneable through the entire green region of the spectrum. U.S. Navy-supported programs to grow laser-quality samples of this material are ongoing at MIT and North American Philips.

The great strides that the fiber optics communications community has made in improving the performance and reliability of near-infrared diode lasers have stimulated U.S. Navy interest in developing frequency-doubled diode laser arrays for ocean-optics applications. Continuous operational lifetimes of 100-1000 years are projected for continuous-wave devices that deliver 10 mW of average IR power at 30 percent efficiency. It is reasonable to speculate that pulsed operation with similar lifetimes, average powers, and efficiencies can be obtained.

In the case of diode lasers, the output pulse length is determined entirely by the drive circuit, so that the two-to-five ns pulses required for hydrography should be readily achievable. Furthermore it is very probable that, by properly choosing diode composition, any frequency-doubled output wavelength in the 480-550 nm range can be obtained.

The main technical problem associated with developing a frequency-doubled diode laser source for hydrography (or for any other ocean-optics application) is that a diode array containing a great many elements must be used to obtain the requisite output energy/pulse. Also, the outputs from many (perhaps a hundred) elements must be phase-locked in order to achieve the power densities necessary for efficient frequency-doubling. For example, in order to realize a hydrographic laser source with 160 kW peak power, an array containing over 10^4 of the best pulsed-laser diodes currently available would be required. While the fabrication of such an array appears to be within the state-of-the-art of integrated circuit technology, it is certainly non-trivial! Also, only a few laser diodes have ever been phase-locked, possibly because there has never before been any motivation to phase-lock hundreds.

A program to investigate the fundamental technical problems associated with frequency-doubled diode laser array development is underway at MIT. It is anticipated that within two years basic feasibility will have been established (or ruled out) so that design and fabrication of a modest-sized (10^3–10^4 element) green radiation source can be initiated.

Summary

A number of new green lasers are presently under development which show promise of satisfying laser hydrography requirements. Some of the most promising of these lasers are listed in Table III, together with comments regarding the status of their development for hydrographic applications. It is probable that if aggressive development efforts were initiated, the first seven entries of Table III could be ready for aircraft-mounted field utilization in one-to-three years. The last four entries in the table would likely require two-to-five years to reach that level of development.

As is implied by Table III, further development of the copper vapor laser shows great promise of providing a significant near-term advancement in the hydrographic source state-of-the-art. One-percent-efficient versions of this device have been available for some time, but their characteristic 20 ns output

Type Laser	Wavelength (nm)	Status
Metallic Copper	511-578	6 kHz, 0.8 mJ/pulse, 20 ns Pulse Length Comm. Available; 8 kHz, 0.7 mJ/pulse, 5 ns Pulse Length Demonstrated
Copper Halide	511-578	Demonstrated Performance Similar to Long Pulse Metallic Cu; Lower Temp. Requirement -- Potential for Long-Life Sealed-Off
Mercury Bromide	490-510	1 mJ/cc/Pulse, 50 ns Operation Demonstrated at 100 Hz; Long Sealed-Off Life Possible; 5 ns pulses possible via Cavity Dump
Mercury Chloride	555-565	Same Potential as Mercury Bromide, but Longer Wavelength
Raman Down-Shifted XeCl	Selectable via Raman Medium	XeCl most Highly Developed MGL; 210 W ave. Dem. in UV; 50% Down Conv. Eff. Achieved with Lead Vapor
UV MGL Pumped Dye	Tuneable in Green	Demonstrated Using KrF and XeF MGL Pumps; Requires Short-Pulse MGL Pump Development
XeF Laser Pumped Tm:YLF	452	Feasibility Demonstrated; Program to Achieve 1 J output in Green Underway
XeCl Laser Pumped Xe_2Cl	478	Demonstrated in Laboratory
Cooled Er:YLF	550	Stimulated Emission Cross-Section Measured at 77° K; High Quality Crystals Grown; Laser Experiment Underway
Room Temp. Ce:ThO_2	Tuneable in Green	Theoretically Promising; Crystal Growth Experiments Underway
Freq.-Doubled Diode Array	Green	Very Long Life, 10% Eff. Appears Possible; 3 ns pulse Length no problem; Exps. to Phase-Lock Many Diodes Underway

Table III. Hydrographic Laser Summary

pulse-length and relatively short operational lifetime have disqualified them for hydrographic applications. This situation has recently been improved by the observation that shorter pulses and longer life can be obtained by operating in a high voltage/low current mode with a high-pressure laser medium.

Over the last several years an entirely new class of near-atmospheric pressure molecular gas lasers has been under development. Some of the most promising of these appear to be highly appropriate for hydrographic application. In particular, it is anticipated that the mercury halide laser systems will be capable of providing wavelength-tuneable outputs in the 500 nm and 570 nm regions of the spectrum, with efficiencies of one percent and pulse energies as high as one joule. Another promising green laser development area involves frequency-downshifting the output of 2-3 percent-efficient UV molecular gas lasers through Stimulated Raman Effect in metal vapors and molecular gases. Fifty percent down-conversion efficiency to the green has already been achieved, and output wavelength selection appears possible. Another technique that has been used successfully to produce intense optical pulses of a type potentially suitable for hydrography is to employ UV output from molecular gas lasers to optically pump gas, dye, and solid-state lasers that operate in the green. Overall efficiencies of one percent appear possible using this approach.

A basic problem associated with the use of molecular gas lasers for hydrography is that these devices generally operate with output pulse lengths of several tens-of-ns. Consequently, special methods must be used to shorten the pulse lengths to the required 3-5 ns range. Programs to apply variants of the "cavity dump" pulse compression technique to these lasers are presently underway, and traveling wave master-oscillator/power-amplifier (MOPA) configurations are being applied to obtain shorter pulses without sacrificing efficiency or output-beam quality. Furthermore, a capacitively pumped, capillary waveguide laser configuration is being investigated which inherently yields short output pulses, while avoiding lifetime problems associated with internal metallic electrodes. This method has been successfully applied to the mercury bromide molecular gas laser as well as to a number of UV producing laser systems.

In addition to the highly developed frequency-doubled Nd:YAG laser, which represents the state-of-the-art in hydrography laser technology, there are a number of advanced solid-state laser options that show great future promise. In particular, there is a good chance that through moderate cooling, several solid-state candidates can be made to operate directly in the green, thus avoiding system complexities associated with frequency-doubling. There is also hope that the great strides in I.R. injection laser reliability, that have been made as a result of fiber-optics communications initiatives, can be exploited to produce a green hydrography laser. Projected injection laser lifetimes of 10^3 years and the likelihood of the development of vastly improved non-linear doubling crystals make the realization of a very long-lived, two-to-five percent-efficient frequency-doubled injection laser for hydrography a very strong possibility for two-to-five years in the future.■

research notes

Marine Fouling on Ships

Drs. James R. Griffith, John D. Bultman, and Donald E. Field of the Naval Research Laboratory (NRL) have developed and successfully tested "fouling release" coatings which allow marine fouling organisms attached to a ship's or a boat's hull to be easily removed by water blasting or wiping by hand.

The non-toxic coatings are composed of powdered poly(tetrafluoroethylene), commonly known as Teflon, dispersed in newly developed fluorinated polyurethane polymers. A conventional airless spray gun can be used to apply the "fouling release" mixture to a hull where after drying it becomes a rugged coating capable of a long-term performance.

In field experiments held at Norfolk, Virginia, the researchers proved that most tenacious marine organisms can be easily removed from hulls coated with "fouling release" by small-stream water blasting or hand wiping . . . even if the ship has been in water for an extended period of time. In one of the Norfolk experiments, NRL scientists using the "fouling release" coatings on the hull of the tug "SEAMULE" were able to quickly remove marine fouling from the boat's hull after it had been in the water for three years. ■

(James R. Griffith, NRL)

More Effective Software Documentation

Significant research results that demonstrate improved human performance on particular types of software documentation techniques have recently been reported by a research team at the General Electric Company headed by Dr. E. Kruesi with the support of the Office of Naval Research. In an experimental test with experienced programmers on the effectiveness of coding from nine format-types for the specifications of a software program, the use of a constrained language format (such as in programming design languages) provided optimal performance in either a sequential or branching arrangement of that format. Such practical measures as time to code and debug, the number of submissions to compile and run the completed code, the number of control flow errors, and the number of editorial commands entered during coding and debugging processes, all supported the effectiveness of the constrained language format. The values of these performance measures increased with the difficulty of the software program problem which ranged upward from an inventory program, to an engineering program, to a data-base query on airport traffic and queuing. Software documentation has been consistently identified as the major source of failure in the control of costs and management of software development; and the phases of software development that are most dependent on good documentation (production, maintenance, optimization and conversion) have created an enormous managerial burden. In a recent Government Accounting Office report (July, 1980), it was estimated from the experience of 33 federal and 25 industrial computer installations that the work done after a program produces its first output accounts for almost 70% of total life-cycle costs and thus, even a small improvement in documentation tools would produce an enormous cost-reduction. ■

(John J. O'Hare, ONR)

Turbulent Mixing In Free Shear Layers

Professors Richard Brown and Anatole Roshko (California Institute of Technology), with research support from the Office of Naval Research, introduced the concept of coherent structures in turbulence and reported the results in a Journal of Fluid Mechanics article published in 1974. Since that time other researchers have shown that the dynamics of mixing (spreading and momentum transfer) in free shear layers is dominated by the pairing of these coherent structures. Very recently, in research supported by ONR, Professor Cheh-Ming Ho (University of Southern California) has experimentally investigated and quantified the relationship between subharmonic flow disturbances and the merging of coherent vortex structures in free shear layers.

Professor Ho develops free shear layers between two coflowing water streams moving at different velocities. Small disturbances at subharmonic frequencies of the fundamental frequency are introduced in one of the streams. Vortex merging and hence mixing are shown to be controlled by the subharmonic frequencies introduced. Theoretically, Professor Ho has shown that some of the properties of the coherent structures and the merging process can be predicted using stability theory.

This research is very valuable in at least two aspects. From a more fundamental view point, that fact that stability theory predicts some of the properties associated with coherent structures offers hope that turbulent flows can be meaningfully studied theoretically. In a more practical sense, the strong influence of small subharmonic disturbances on coherent structures may have such applications as controlling mixing in internal combustion flows or reducing turbulent friction in external flows. ■

(Robert E. Whitehead, ONR)

ONR Contractors Accomplish Breakthrough in Electronic Localization Problem

In 1958, P. W. Anderson formulated a famous problem that eventually lead to his Nobel Prize: consider an electron with energy E moving in a spatially random potential. Is the electron able to move through essentially all of space, i.e., is it extended, or is it localized in some region of space where the potential is particularly attractive? This question has direct relevance to the nature of electrical conduction in random and amorphous materials. If electrons are localized in a random potential, they will not conduct. Anderson concluded that for low energies the electron would be localized and that at high energies it would conduct, the localized and conducting regions being separated by a mobility edge at energy E_m. He was, however, unable to provide any proof of the existence of, or calculate electronic properties in the vicinity of the mobility edge.

Over the years, considerable effort has been devoted to understanding this problem. There have been many numerical calculations and many attempts to produce approximate analytic solutions. Neither, however, produced convincing results. Over the past ten years, a great deal has been learned about another complicated problem, critical fluctuations in the vicinity of second order phase transitions. In particular, it was learned that it is very fruitful to study this problem as a continuous function of spatial dimension d. In high dimension, the solution is given by mean field theory and is "trivial". Below some critical dimension, d_c, (usually 4), however, the problem becomes much more complicated. Calculations for d just below d_c can be carried out, however, and they yield valuable information about the structure of the theory in physical dimensions, $d = 2$ and 3.

At the University of Pennsylvania, Professors A. B. Lubensky and T. C. Harris, under Office of Naval Research contract, have studied the localization problem using the phase transition problem as a guide. They have found a mean field theory valid above eight dimensions, yielding localized and extended states and a mobility edge, and have calculated properties in the vicinity of the mobility edge just below eight dimensions. They are able to extend their results to lower dimensions, finding that $d = 4$ emerges as another critical dimension, below which the nature of the mobility edge changes. They point out that their solution to the mobility edge problem is almost identical to another problem, the statistics of branched polymers in solutions.

This work on the localization problem seems to be of fundamental importance. It is the first complete solution to this problem in any dimension. The structure of the solution for $d > 4$ is totally different from what was generally believed, and is probably a prototype for a whole class of problems that have not as yet been investigated. It is important to note that mean field theory is used very extensively in physics because of its simplicity, and because it generally gives qualitatively correct results. In the case of the localization problem, they find that mean field theory

is qualitatively correct only above d = 4 and should not be used at all for d = 2 or 3. The total problem is by no means solved, and remains one of the most active and important areas of research in solid state physics. ■

(George B. Wright, ONR)

New Understanding of the Links Between Bacterial Films and Larval Settlement

Dr. Ralph Mitchell and David Kirchman of Harvard University, ONR contractors of the Oceanic Biology Program, have made a breakthrough concerning the connection between microbial films which form on surfaces introduced into the marine environment, and the settlement and metamorphosis of larvae of one fouling organism, the tube-building polychaete *Janua brasiliensis*. In tests using films made of pure bacterial cultures, *Pseudomonas marina* was shown to be particularly active in inducing larval settlement. *Pseudomonas* films were even stimulatory after being formalin-killed. It was then shown that the polychaete larvae only settled on the extracellular polymer (capsule) produced by the bacteria. It was hypothesized that the polymer elicited a response from specific polysaccharide-binding proteins, known as lectins, on the larval surface. The lectin binding sites on the bacterial polymer were then experimentally blocked. This prevented larval settlement. The hypothesis was further tested by pre-treating the larvae in a manner to block the larval lectins. This also prevented settlement. These data show that:

a. Specific bacteria induce settlement of *Janua* larvae

b. Extracellular bacterial polymers are responsible for settlement

c. The larvae produce binding proteins (lectins) that attach specifically to the bacterial polymers

d. The lectins can be blocked by flooding the larval surface with specific carbohydrates ■

(Peter A. Jumars, ONR)

Deep Levels in III-V Alloy Semiconductors

The properties of semiconductor materials are dominated by impurity effects. So-called shallow energy levels for electrons are very close in energy to the conduction band edge energies. Physically, they are pictured as electrons very weakly bound to the impurity and easily excited into a free electron conduction band state. Of increasing interest are the "deep levels" produced by impurities (donor or acceptor) which differ from the band edge energies by 0.1 electron volts or more. Further, the electron in such a state is bound close to the impurity (localized) and is thus more susceptible to lattice atom motion (phonons), position (configurational effects on Coulomb energy), and excitonic effects. Since such deep levels play important roles on carrier scattering and carrier lifetime, their effects on electron devices have become more important as more sophisticated devices and materials have been developed and as devices get smaller.

The microscopic characterization of deep level states is a very difficult and challenging problem, but some recent results by an Office of Naval Research contractor, Dr. Donald Wolford at IBM, have given new understanding to deep level states in III-V alloy semiconductors. Part of the work was done at Illinois while he was a student.

The new results arise when careful light scattering experiments were carried out using tunable dye-laser-excited Resonance Raman Scattering (RRS) on nitrogen doped GaAs(1-x)P(x) in which X is variable. Luminescence line shapes can be analyzed in terms of broadening due to random alloy disorder effects on local (defect) Coulomb energies (i.e. inhomogeneous broadening). The broadening increases with increasing alloying (x increasing), implying increased localization of the electron state, and it peaks near X = .50. Verification of the energy states of nitrogen as being a deep level were made by showing that the energy is independent of the nearby conduction band. Again using RRS, excitonic substructure is found on the deep trap which is due to electron-hole exchange energy which splits the exciton into two sublevels. The conclusion is that electron localization at the nitrogen impurity is dependent on binding energy and varies continuously with the alloying parameter X, and also that the large amount of exchange energy suggests a very compact charge density. These results are important to our understanding of deep levels and our ability to study and use them in preparing new materials and devices. ■

(Larry R. Cooper, ONR)

DEPARTMENT OF THE NAVY
OFFICE OF NAVAL RESEARCH
ARLINGTON, VA. 22217

OFFICIAL BUSINESS
PENALTY FOR PRIVATE USE, $300

POSTAGE AND FEES PAID
DEPARTMENT OF THE NAVY
DOD-316
CONTROLLED CIRCULATION RATE